Knockdown of Virus Antigen Expression Increases Therapeutic Vaccine Efficacy in High-titer HBV Carrier Mice

Short title: siRNA enables therapeutic hepatitis B vaccination

Authors

Thomas Michler[1,10] *, Anna D. Kosinska[1,10] *, Julia Festag[1], Till Bunse[1,10], Jinpeng Su[1], Marc Ringelhan[1,2], Hortenzia Imhof[1], Dirk Grimm[3,10], Katja Steiger[4], Carolin Mogler[4], Mathias Heikenwalder[5], Marie-Louise Michel[6], Carlos A. Guzman[7,10], Stuart Milstein[8], Laura Sepp-Lorenzino[8], Percy Knolle[9,10], Ulrike Protzer[1,10]

* the authors contributed equally to the work

Affiliations

[1]Institute of Virology, Technical University of Munich / Helmholtz Zentrum München, Trogerstrasse 30, D-81675 Munich, Germany.

[2]Department of Internal Medicine II, University Hospital rechts der Isar, Technical University of Munich, Ismaninger Str. 22, D-81675 Munich, Germany.

[3]Department of Infectious Diseases/Virology, Heidelberg University Hospital, BioQuant, Im Neuenheimer Feld 267, D-69120 Heidelberg, Germany.

[4]Institute of Pathology, Technical University of Munich, Trogerstrasse 18, D-81675 Munich, Germany.

[5]Division of Chronic Inflammation and Cancer, German Cancer Research Center (DKFZ), Im Neuenheimer Feld 242, D-69120 Heidelberg, Germany.

[6]Institut Pasteur, 28 rue Dr Roux, 75015 Paris, France.

[7]Department of Vaccinology and Applied Microbiology, Helmholtz Centre for Infection Research, Inhoffenstr. 7, D-38124 Braunschweig, Germany.

[8]Alnylam Pharmaceuticals, 300 Third Street, Cambridge, MA 02142, USA.

[9]Institute of Molecular Immunology, University Hospital rechts der Isar, Technical University of Munich, Ismaninger Strasse 22, D-81675 Munich, Germany.

[10]German Center for Infection Research (DZIF), Munich, Heidelberg and Hannover/Braunschweig partner sites, Germany.

Author contributions

TM, AK and UP designed the study; AK, HJ, TB, JS and TM performed experiments; MLM, JH, TM and DG developed AAV vectors and the mouse model; AK and UP established the vaccination scheme; TM, MR, KS, MH and CM performed histological analyses; TM, AK, PK and UP analyzed and interpreted data and wrote the manuscript. All authors confirmed the final version of the manuscript.

Grant support

The study was funded by the Deutsche Forschungsgemeinschaft (DFG, German Research Foundation), project No. 272983813, via the Transregional Collaborative Research Center TRR179 (to UP, DG, PK and MH) and by funds of the Helmholtz Association via the Helmholtz-Alberta Initiative on Infection Diseases (HAI-IDR to CAG and UP). TM received a clinical leave stipend, and TB obtained a MD thesis stipend from the Academy of the German Center for Infection Research (DZIF).

Abbreviations

AAV, Adeno-Associated Virus; GalNAc, N-acetylgalactosamine; i.m., intramuscular; i.v, intravenous; MVA, Modified Vaccinia Ankara virus; pgRNA, pregenomic RNA; RNAi, RNA interference; s.c., subcutaneous; shRNA, short hairpin RNA; siCtrl, Control siRNA; siHBV, HBV siRNA; siRNA, small interfering RNA; TherVacB, therapeutic hepatitis B vaccine

Financial Disclosures

SM is and LSL was an employee of Alnylam Pharmaceuticals. The work was supported by a research grants from Alnylam Pharmaceuticals and VIR Biotechnology. TM and UP are *ad hoc* scientific advisors to VIR Biotechnology, a licensee of the HBV-specific siRNA technology. CAG is named as inventor in a patent covering the use of c-di-AMP as adjuvant (PCT/EP2006/010693). UP and AK are named as inventors on a patent application describing the therapeutic vaccination scheme of TherVacB (PCT/EP2017/050553). UP, TM and LSL are named as inventors on combining siRNA with therapeutic vaccination (PCT/EP2018/028116). DG is a co-founder and shareholder of AaviGen GmbH, UP a co-founder and shareholder of SCG Cell Therapy. The remaining authors declare no competing interests.

Correspondence: Prof. Ulrike Protzer, Institute of Virology, Technical University of Munich / Helmholtz Zentrum München, Trogerstrasse 3, D-81675 Munich, Germany. e-mail: protzer@tum.de; protzer@helmholtz-muenchen.de, Tel.: +49 (0)89 4140-6886; Fax: - 6823

Abstract (edited version)

Background & Aims: Hepatitis B virus (HBV) infection persists because the virus-specific immune response is dysfunctional. Therapeutic vaccines might be used to end immune tolerance to the virus in patients with chronic infection, but these have not been effective in patients. In patients with chronic HBV infection, high levels of virus antigens might prevent induction of HBV-specific immune responses. We investigated whether knocking down expression levels of HBV antigens in liver might increase the efficacy of HBV vaccines in mice.

Methods: We performed studies with male C57BL/6 mice that persistently replicate HBV (genotype D, serotype ayw)—either from a transgene or after infection with an adeno-associated virus that transferred an overlength HBV genome—and expressed HB surface antigen (HBsAg) at levels relevant to patients. Small hairpin or small interfering (si)RNAs against the common 3'-end of all HBV transcripts were used to knock-down antigen expression in mouse hepatocytes. siRNAs were chemically stabilized and conjugated to N-acetylgalactosamine to increase liver uptake. Control mice were given either entecavir or non-HBV specific siRNAs and vaccine components. Eight to twelve weeks later, mice were immunized twice with a mixture of adjuvanted HBV S and core antigen, followed by a modified vaccinia virus Ankara vector to induce HBV-specific B- and T-cell responses. Serum and liver samples were collected and analyzed for HBV-specific immune responses, liver damage, and viral parameters.

Results: In both models of HBV infection, mice that express hepatocyte-specific small hairpin RNAs or that were given subcutaneous injections of siRNAs had reduced levels of HBV antigens, HBV replication, and viremia (1–3 $\log_{10}$ reduction), compared to mice given control RNAs. Vaccination induced production of HBV-neutralizing antibodies, and increased numbers and functionality of HBV-specific, CD8+ T-cells in mice with low, but not in mice with high levels of HBV antigen. Mice with initially high titers of HBV and knockdown of HBV antigen expression, but not mice with reduced viremia following administration of entecavir, developed polyfunctional, HBV-specific CD8+ T cells and HBV was eliminated.

Conclusions: In mice with high levels of HBV replication, knockdown of HBV antigen expression along with a therapeutic vaccination strategy, but not knockdown alone, increased numbers of effector T cells and eliminated the virus. These findings indicate that high titers of virus antigens reduce the efficacy of therapeutic vaccination. Anti-HBV siRNAs and therapeutic vaccines are each being tested in clinical trials—their combination might cure chronic HBV infection.

Keywords

Viral hepatitis, immunization, siRNA, immunotherapy, immune tolerance

Main Text

Chronic HBV infection affects 260 million humans and causes 880,000 deaths per year[1] with still rising numbers[2]. Current treatment options are nucleos(t)ide analogues (NUC) that efficiently control HBV replication, reduce liver inflammation and limit progression of liver pathology, but do not affect virus persistence. More importantly, such treatment leaves infected individuals at risk to develop hepatocellular carcinoma[3]. Treatment with interferon alpha can be curative in a low number of patients by influencing the activation status of different immune cells[4] and by its antiviral activity, e.g. by inducing degradation of the viral persistence form, HBV cccDNA[5], but has severe side effects. In the absence of a curative antiviral therapy, induction of protective antiviral B- and T-cell responses either by deliberate stimulation of innate or adaptive immunity or by spontaneous immune recovery after antiviral therapy are essential to cure HBV infection.

How HBV prevents successful immune control remains unclear. While HBV-specific CD8 T cells are key to limit acute HBV infection[6], HBV persistence is characterized by scarcity and dysfunction of virus-specific T cells[7] and by a lack of neutralizing antibodies. Spontaneous immune control is observed in 0.5% chronically infected patients[8] with neutralizing antibodies and HBV-specific CD4 and CD8 T-cell responses becoming detectable. Although prophylactic vaccination using recombinant hepatitis B surface antigen (HBsAg) very efficiently induces neutralizing antibodies, attempts to establish a therapeutic vaccine breaking immune tolerance in chronic hepatitis B have failed so far[9, 10]. We reasoned that the extraordinarily high levels of viral antigens may contribute to HBV-specific immune tolerance and decided to explore the potential of RNAi to control hepatic HBV-antigen expression to render therapeutic hepatitis B vaccination more successful in particular in high-antigenemic HBV carriers.

To improve therapeutic vaccination, we developed a therapeutic hepatitis B vaccination scheme, TherVacB, which employs a heterologous prime-boost strategy[11]. A protein prime using particulate, recombinant HBsAg and HBV core antigen and an adjuvant allowing an activation of B and T cell responses is designed to induce antibodies that capture viral antigens and prevent

virus spread, and to prime CD4 and CD8 T cells. A vector-boost vaccination using modified vaccinia virus Ankara (MVA) expressing HBV envelope and core proteins shall amplify HBV-specific B- and T-cell responses.

To evaluate the effect of viral antigen levels on vaccine efficacy, we used two murine immune-competent models of persistent HBV infection: HBV-transgenic mice reflecting vertical transmission from mother to child[12], and the Adeno-associated virus (AAV)-HBV model in which adult mice develop persistent HBV infection[13]. In this study, we demonstrate that reducing HBV antigen expression by RNAi enabled a therapeutic, heterologous prime-boost vaccine to control and finally eliminate HBV in high-antigenemic carrier mice.

Material and methods

Ethical statement and animal experimentation. HBsAg levels from patient sera were measured between May 2011 and June 2017 as part of clinical routine patient care and are summarized in Figure 1*A* after approval by the ethics committee of the University Hospital rechts der Isar of the Technical University of Munich (approval No. 621/19 S). Animal experiments were conducted in strict accordance with the German regulations of the Society for Laboratory Animal Science (GV-SOLAS) and the European Health Law of the Federation of Laboratory Animal Science Associations (FELASA). Experiments were approved by the local Animal Care and Use Committee of Upper Bavaria (permission number: 55.2-1-54-2532-202-12) and followed the 3R rules. Mice were kept in a specific-pathogen-free (SPF) facility under appropriate biosafety level following institutional guidelines. The experiments were performed during the light phase of the day.

Animal models. HBV-transgenic (HBVtg) HBVxfs male mice, carrying a 1.3-fold overlength HBV genome (genotype D, serotype ayw) on a C57BL/6J background [haplotype H-$2^{b/b}$]$_{12}$, were selected to express high HBsAg levels between 10^3 and 10^4 IU/ml and HBeAg levels ≥200 PEI U/ml. Treatment was started at age 8 to 12 weeks, and litter mates were distributed throughout experimental groups. Alternatively, persistent HBV replication was established by intravenous injection of an Adeno-associated virus (AAV) serotype 2 genome encoding a 1.2-fold overlength HBV genome (AAV-HBV) of genotype D and pseudotyped with an AAV serotype 8 capsid[13] into 8-weeks-old male C57BL/6J mice (Charles River Laboratories, Schulzfeld, Germany). AAV-HBV dose was established by a titration experiment and selected to reach HBsAg levels detected in the majority of our HBV-infected patients (Figure 1*A*). Animals were bled one day before start of treatment and allocated into age-matched groups with similar HBsAg and HBeAg levels. According to animal protection law, each experiment was performed once.

Therapeutic hepatitis B vaccine (TherVacB). Mice were immunized with a heterologous protein-prime / recombinant Modified Vaccinia Ankara virus (MVA) vector-boost vaccination scheme, as described[11]. Briefly, mice were immunized intramuscularly (i.m.) twice with 15 µg of particulate HBsAg (genotype A, adw) expressed in yeast and 15 µg of HBV core protein (genotype D, ayw) particles purified from *E. coli* (kindly provided by APP Latvijas Biomedicinas, Riga, Latvia) adjuvanted with 10 µg cyclic di-adenylate monophosphate (c-di-AMP) (InvivoGen, San Diego, CA, USA). Two weeks after the second protein vaccination, mice were boosted by i.m. injection of $5x10_7$ plaque-forming units (PFU) each of recombinant MVA vectors expressing HBV S or HBV core protein (both genotype D, ayw). Control vaccination consisted of two i.m. injections of the adjuvants without HBV proteins and a boost with an MVA not expressing any transgene. Mice were sacrificed one week (HBVtg mice) or 18 weeks (long-term efficacy study in AAV-HBV model) after MVA boost immunization. Blood and organs were collected for further analysis.

Suppression of HBV-antigen expression by HBV-specific RNA interference (RNAi). Self-complementary AAV vectors co-expressing a H1 promoter-driven shRNA designed to target the common 3'-end of all HBV transcripts together with a U6 promoter-driven cognate shRNA sense strand decoy ("TuD") were pseudotyped with a serotype 8 capsid and purified to generate AAV-shHBV (described before as shHBV7/TuDHBV7)[14]. AAV-shCtrl (described before as shα1AT/TuDα1AT[14]) encodes a shRNA targeting human α_1-antitrypsin and the respective decoy. Per vector, $1x10_{11}$ genome equivalents (geq) were injected intravenously (i.v.).

Stabilized, liver-targeted siRNAs were chemically modified and conjugated to N-acetylgalactosamine (GalNAc) to increase their stability and liver uptake[15]. HBV-specific siRNAs (siHBV1 and siHBV2) were designed to target the common 3'-end of all HBV transcripts. The Control siRNA (siCtrl) targeted human α_1-antitrypsin. Three mg/kg body weight of GalNAc-siRNAs were injected subcutaneously (s.c.) every 4 weeks.

NUC therapy. For antiviral treatment, HBVtg mice received 1 µg/ml Entecavir (ETV, Baraclude™ oral suspension; Bristol-Myers Squibb, Munich, Germany) in drinking water throughout the experiment.

Detection of HBV-specific T cells by MHC class I multimers and intracellular cytokine staining. Splenocytes and liver-associated lymphocytes (LAL) were isolated and LAL were purified by density gradient centrifugation and stained with MHC class I multimers as described[11]. Multimers conjugated with K_b-restricted HBV-derived peptides $S_{190-197}$ (S_{190}; VWLSAIWM), $core_{93-100}$ (C_{93}; MGLKFRQL), MVA-derived peptide $B8R_{20-27}$ (MVA_{B8R}; TSYKFESV) and as control ovalbumin-derived peptide $S8L_{257-264}$ (OVA_{S8L}; SIINFEKL) were kindly provided by Dirk Busch (Technical University of Munich, Germany). Per sample, 0.4 µg multimer was labeled with 0.4 µl Streptactin-PE (IBA Lifesciences, Göttingen, Germany) in 30 µl FACS buffer and incubated for 30 min on ice before adding to the cells.

For intracellular cytokine staining, CD8 T cells were stimulated overnight in the presence of 1 mg/ml Brefeldin A (Sigma-Aldrich, Taufkirchen, Germany). For stimulation, either 1 µg/ml of the indicated synthetic peptide MVA_{B8R}, OVA_{S8L} and HBV S_{190}, C_{93} or $S_{208-215}$ (S_{208}; IVSPFIPL) or peptide pools covering HBV core (genotype D, aa 70-157) or S (genotype D, aa 145-226) containing the dominant CD8 as well as CD4 T-cell epitopes were used.

Cell-surface staining was performed using anti-CD8 (clone 56.6-7; BD Biosciences, Heidelberg, Germany), anti-CD4 (clone L3T4; BD Biosciences), anti-PD1 (clone J43; Invitrogen) and anti-TIM3 (clone B8.2C12; BioLegend) antibodies. Dead cells were excluded from analysis by ethidium monoazidebromide (Invitrogen, Karlsruhe, Germany) or fixable viability dye eF780 (eBioscience, Frankfurt, Germany) staining. Intracellular cytokine staining was performed as described previously[11] using an anti-IFNγ antibody (clone XMG1.2; eBioscience) and anti-TNF antibody (clone: MP6-XT22; BD Biosciences). Data were acquired on a FACSCanto II™ (BD Biosciences) or a CytoflexS (Beckmann Coulter) flow cytometer and analyzed using FlowJo software (Tree Star, Ashland, OR, USA). Gating strategy of flow cytometric analysis is presented

in Supplementary Figure 7. Data from multimer and intracellular cytokine staining are presented as relative values after background subtraction determined using OVA_{S8L} peptide. Absolute T-cell numbers per liver or spleen were determined using CountBright absolute counting beads (Invitrogen, Karlsruhe, Germany) according to the manufacturer's instructions.

Serological analyses. Serum HBsAg, HBeAg and anti-HBs levels were quantified on an Architect™ platform after dilution with the Architect HBsAg Manual Diluent (lowest dilution 1:5) using the quantitative HBsAg test (Ref.: 6C36-44; Cutoff: 0.25 IU/ml), the HBeAg Reagent Kit (Ref.: 6C32-27) with HBeAg Quantitative Calibrators (Ref.: 7P24-01; Cutoff: 0.20 PEI U/ml) and the anti-HBs test (Ref.: 7C18-27; Cutoff: 12.5 mIU/ml) (all Abbott Laboratories, Wiesbaden, Germany), respectively. Anti-HBe levels were determined after 1:6 dilution in phosphate-buffered saline (PBS) plus 10% fetal calf serum (FCS) using the Enzygnost™ anti-HBe monoclonal test (data given in Relative Light Units [RLU] with >0.832 RLU considered negative) on the BEPIII platform (Siemens Healthcare, Eschborn, Germany). Serum alanine aminotransferase (ALT) activity was measured in a 1:4 dilution in PBS using the Reflotron® GPT/ALT test (Roche Diagnostics, Mannheim, Germany). Values and cutoffs of quantitative tests are given after correction for the respective dilution.

Analysis of HBV DNA in serum and liver. DNA was extracted from 25 µl of serum using the QIAamp MinElute Virus Spin Kit (Qiagen, Hilden, Germany) according to the manufacturer's protocol and eluted into 50 µl H_2O. For qPCR analysis from liver tissue, DNA was extracted using the NucleoSpin Tissue kit (Macherey-Nagel, Düren, Germany). Quantitative HBV-specific real-time PCR (lower limit of quantification [LLOQ]: 1.705 copies / µl serum) was performed on an Applied Biosystems® 7500 Real-time PCR system (Thermo Fisher Scientific, Darmstadt, Germany) using primers HBV1464_fw / HBV1599_rev and a Taqman probe. To determine HBV genome copy numbers per cell in the transgenic mouse model, numbers of diploid cell genomes were subtracted as the HBV-specific PCR also amplifies the HBV integrate. Values determined for HBV genome copy numbers per cell in the AAV-HBV model were corrected for the AAV-HBV

by subtracting AAV-copies using AAV_ITR primers. Cell numbers were determined by real-time PCR for the single-copy mouse prion protein gene (mPrp). For primer/probe sequences and cycling conditions, see Supplementary Table 1. For Southern blot analysis, frozen liver samples were lysed using the Tissue Lyser LT (Qiagen), and after adding 20% SDS and digestion with proteinase K and RNase A, DNA was extracted with phenol-chloroform. Equal amounts of DNA extracted from individual animals within the same treatment group were pooled, digested overnight with *Hind III* (Thermo Fisher Scientific), separated through a 1.0% agarose gel, transferred onto a nylon membrane and UV cross-linked prior to overnight hybridization with a digoxigenin-labeled DNA probe at 65°C. HBV-DNA was visualized using the DIG Luminescent Detection kit (Roche Diagnostics) on an ECL Chemocam (INTAS Science Imaging Instruments, Göttingen, Germany).

Analysis of HBV transcripts. RNA was extracted from livers using the RNeasy Mini kit (Qiagen). cDNA was reverse transcribed using the SuperScript III kit (Thermo Fisher Scientific) and HBV transcripts were amplified by real-time RT-PCR on a LightCycler® 480 Instrument II (Roche Diagnostics) with primers to detect only HBV 3.5 kb transcripts that mainly consist of HBV pregenomic RNA. Results were normalized to expression of Glyceraldehyde 3-phosphat dehydrogenase (GAPDH). For primer sequences and cycling conditions, see Supplementary Table 1.

Histology and immunohistochemistry. Livers were fixed in 4% buffered formalin for 48 h, dehydrated and embedded in paraffin before serial 2 µm-thin sections were prepared. Hematoxylin-Eosin (HE) staining was performed on deparaffinized sections with Eosin and Mayer´s Haemalaun according to standard protocols. Histopathological evaluation was performed by an experienced liver pathologist in a blinded manner. A general description of histopathological findings was provided as well as a grading system including severity of inflammation, necrosis and fibrosis ranging from 0 (=none) to 3 (=very strong). For immunohistochemistry, rabbit anti-CD3 (Zytomed Systems GmbH, Berlin, Germany; #RBK024-05; 1:250 dilution; retrieval at 95°C

for 30 min with EDTA), rat anti-CD4 (eBioscience, Frankfurt a. Main, Germany; #14-9766-82; 1:1,000 dilution; retrieval at 100°C for 30 min with EDTA) or rabbit anti-HBV core (Diagnostic Biosystems, Pleasanton, CA, USA; #RP 017; 1:50 dilution; retrieval at 100°C for 30 min with EDTA) were used on a Leica Bond MAX system (Leica Biosystems, Nussloch, Germany). Anti-CD8 stains were performed on cryo-conserved tissue using rat primary anti-CD8 (BD Bioscience; #553027; 1:200 dilution). For analysis, tissue slides were scanned using a SCN 400 slide scanner (Leica Biosystems). Positive cells were quantified from at least three tissue areas adding up to ≥10 mm^2 using the integrated Tissue AI software (Leica Biosystems).

Statistical analyses. Statistical analyses were performed using GraphPad Prism version 6.0. Data sets were initially analyzed for Gaussian distribution with D'Agostino-Pearson omnibus test. Depending on the results, parametric student t test, 1- or 2-way Anova with Tukey´s, Dunnett´s or Sidak´s multiple comparison correction or non-parametric Mann-Whitney U or Kruskal-Wallis with Dunn´s multiple comparison correction tests were used. Linear regression was analyzed using two-tailed Pearson correlation. *p*-values <0.05 were considered significant.

Results

HBV antigen titers determine the antiviral effect of therapeutic vaccination.

In sera of 354 patients sent in for routine HBsAg quantification, the majority of HBsAg titers were between 10^3 and 10^4 IU/ml (Figure 1*A*) matching titers observed in other clinical cohorts[16, 17]. These levels exceeded HBsAg levels in mice used in previous studies evaluating therapeutic vaccination[11] by ≥ 2log10. To investigate the effect of clinically relevant antigen levels on the induction of HBV-specific immune responses, we chose HBV-transgenic mice with HBsAg levels of 10^3-10^4 IU/ml and reduced antigenemia by RNAi using an AAV vector expressing a shRNA that targets all HBV transcripts (shHBV)[14]. AAV-shHBV stably suppressed HBsAg and hepatitis B e antigen (HBeAg) levels and viremia by 1-2 $\log_{10}$ (Figure 1*B*-*D*), but neither antibodies against HBsAg (anti-HBs; Figure 1*E*) nor antibodies against HBeAg (anti-HBe, data not shown) became detectable.

Eight weeks after AAV-shRNA application, heterologous protein prime - MVA vector boost vaccination scheme TherVacB was initiated. TherVacB, but not control vaccination, reduced HBsAg and viremia by 1-2$\log_{10}$ (Figure 1*B*,*D*; Supplementary Figure 1*A*-*C*) and induced high titers of anti-HBs (Figure 1*E*; Supplementary Figure 1*D*) in all animals. Without shHBV pretreatment, however, TherVacB failed to reduce HBeAg levels when applied to mice replicating HBV at high levels (Figure 1*C*; Supplementary Figure 1*B*,*E*). Strikingly, TherVacB after shHBV was able to reduce HBsAg, HBeAg and viremia significantly to levels hardly detectable (Figure 1*B*-*D*).

To compare the antiviral effect of either treatment, we analyzed HBV gene expression and replication in the liver. Cytoplasmic staining of HBV core protein that reflects active viral replication[18] was reduced in hepatocytes of mice expressing shHBV but dropped even further after TherVacB (Figure 1*F*,*G*). Southern blot and PCR analyses revealed that both, shHBV and TherVacB reduced HBV replication while sequential application of shHBV and TherVacB – except in one animal – was able to completely stop it (Figure 1*H*,*I*). Thus, reducing HBV antigen

expression by RNAi enabled therapeutic vaccination to efficiently control HBV.

Therapeutic vaccination triggers T-cell infiltration into the liver.

After vaccination, only those HBV-transgenic animals that were pretreated with shHBV before TherVacB showed a moderate, two-fold increase of serum alanine transaminase (sALT) activity (Supplementary Figure 2*A*). We therefore analyzed liver biopsies of animals from the different treatment groups for the infiltration of T cells by immunohistochemistry staining of CD3, CD4 and CD8 (Figure 2*A*-*C*). Matching the sALT increase, T cell infiltration was most pronounced in animals starting to express shHBV before TherVacB (Figure 2*A*). While all animals that received TherVacB showed a T-cell infiltration into the liver, this was not the case in animals that solely expressed shRNA (Figure 2*C,* Supplementary Figure 2*B*). CD4 T cells were detected in similar numbers in all TherVacB-treated animals irrespective of shRNA expression. However, only animals that expressed shHBV before receiving vaccination showed a significantly stronger CD8 T-cell infiltration (Figure 2*B*,*C*). Therapy with AAV-shHBV as well as TherVacB was well tolerated, and neither was associated with histopathological changes (Figure 2*D*).

From these results we concluded that reducing virus and antigen load by RNAi neither activates antibody responses nor T-cell infiltration into the liver. TherVacB is able to induce antibody responses, and RNAi combined with therapeutic vaccination resulted in a CD8 T-cell infiltration into the liver.

HBV-specific shRNA enables TherVacB to induce HBV-specific CD8 T-cell responses.

Lowering HBV-antigen expression in HBV-transgenic mice by shHBV enabled TherVacB to break HBV-specific immune tolerance and to induce a more prominent HBV-specific effector CD8 T-cell response than delivery of a control shRNA (shCtrl) (Figure 3*A*-*F*). TherVacB alone activated HBV-specific CD4 T cells that could be detected in liver and spleen, but was only able to induce a minor

HBV-specific CD8 T-cell response (Figure 3*A,C,D,* Supplementary Figure 3*A*). MVA-specific T-cell responses were equally strong in all vaccinated groups (Figure 3*A,B*) proving that CD8 T-cell tolerance is induced by HBV antigens and is specific for HBV.

Reducing virus and antigen load by RNAi neither on its own (Figure 3*A,C*) nor in combination with stimulating innate immunity by control vaccination (Supplementary Figure 3*B*) resulted in activation of HBV-specific CD4 or CD8 T-cell responses. Only the combination of shHBV and TherVacB led to profound hepatic HBV S- and core-reactive, polyfunctional CD8 T-cell immunity (Figure 3*E*,*F*) proving that antigen-specific immune activation was required to induce HBV-specific immunity. A mild elevation of serum ALT activity indicated a cytotoxic effector function of HBV-specific T cells *in vivo* (Figure 3*G*). Overall, high serum HBV-antigen levels (HBsAg>500 IU/ml, HBeAg > 200 PEI U/ml) at the start of therapeutic vaccination negatively correlated with the ability to mount HBV-specific CD8 T-cell responses (Figure 3*H*,*I*). Taken together, our results indicate that CD8 T cells induced by TherVacB can overcome HBV-specific immune tolerance and control HBV replication without prominent liver damage, but only when HBV-antigen expression is low, e.g. after suppression by RNAi.

In contrast to nucleoside analogues, RNAi enables TherVacB to break HBV-specific immune tolerance.

To facilitate clinical translation of sequential RNAi and therapeutic vaccination, we developed GalNAc-conjugated siRNAs that target hepatocytes following s.c. application[15] and are optimized to silence all HBV transcripts and to inhibit HBV replication. Two different HBV-siRNAs (siHBV1 and siHBV2) were selected. Monthly s.c. injections of siHBV1 or siHBV2 lowered serum HBsAg by 2 $\log_{10}$, HBeAg by 1 $\log_{10}$ and viremia by 1-2 $\log_{10}$, which was comparable to the effect observed with continuous expression of shHBV by the AAV vector in HBV-transgenic mice (Figure 4*A*-*D*). No antiviral effect was observed after application of the control siRNA (siCtrl). The standard-of-care oral nucleoside analogue Entecavir inhibited HBV replication and reduced HBV

viremia to undetectable levels (Figure 4*C*), but did not affect HBsAg or HBeAg levels (Figure 4*A*,*B*). Again, TherVacB induced seroconversion to anti-HBs (>1,000 IU/ml) irrespective of pre-treatment (Supplementary Figure 4*A*) and consistently reduced HBsAg levels and viremia (Figure 4*A*,*D*), but did not reduce HBeAg (Figure 4*B*). Importantly, after siHBV- or shHBV-mediated RNAi, but not in Entecavir-treated animals, TherVacB generated high numbers of functionally active, HBV-specific CD8 T cells (Figure 4*E*; Supplementary Figure 4*B*), controlled HBV-core expression in hepatocytes (Figure 4*F*,*G*) and reduced HBV-DNA in the liver to undetectable levels in all but two animals (Figure 4*H*). MVA-directed CD8 T-cell responses were not affected by any pre-treatment (Supplementary Figure 4*C*). None of the treatment combinations induced significant liver damage (Supplementary Figure 4*D*). This demonstrates that reducing HBV-antigen expression is necessary to allow TherVacB to break HBV-specific immune tolerance and control HBV replication while inhibiting HBV replication is not sufficient.

Combination of siHBV with TherVacB achieves sustained control of HBV in AAV-HBV-infected mice.

To finally evaluate the potential of siHBV in combination with TherVacB to achieve a “cure” of HBV, we employed the AAV-HBV model of chronic HBV infection, in which HBV-specific immune tolerance develops and HBV replication persists for several months[13]. In AAV-HBV-transduced mice the nuclear HBV-transcription template remains episomal[19, 20] and can be lost and - in contrast to HBV-transgenic mice - HBV-replicating hepatocytes can be eliminated.

We infected mice with ascending amounts of AAV-HBV (Figure 5*A,B*) to achieve stable antigen titers at different levels and, four weeks later, vaccinated the same mice with TherVacB. TherVacB controlled HBV only in mice expressing low- but not in those expressing high-level HBV-antigens (Figure 5*A,B*). This correlated with the induction of HBV-specific immune responses. Anti-HBs was induced in all animals. However, anti-HBs titers as well as HBV-specific CD8 T-cell responses inversely correlated with HBV antigen titers, and were not detected anymore in mice expressing

HBV at high levels (Figure 5*C,D*). This demonstrated that in AAV-HBV-infected mice, HBV-specific T-cell tolerance was already established after four weeks.

To investigate whether pretreatment with siRNA may enable TherVacB to cure higher-titer HBV carriers, we infected a new set of mice with AAV-HBV to establish persistent HBV replication with HBsAg levels detected in the majority of patients in Western countries (10^3-10^4 IU/ml, see Figure 1*A*). Four weeks after AAV-HBV infection, when HBV-specific T-cell tolerance was established (Figure 5*A-D*), siHBV1, siHBV2 or siCtrl were injected three times at four-weekly intervals and TherVacB was initiated together with the last siRNA dose. siHBV1 and siHBV2 rapidly reduced HBsAg by 2-3$\log_{10}$ and HBeAg by ≥1$\log_{10}$ (Figure 5*E-F*). All TherVacB-vaccinated animals developed anti-HBs (Figure 5*G*) and showed a moderate, maximally 1$\log_{10}$ drop in HBsAg. Again, HBV-specific siRNAs alone failed to trigger HBV-specific immunity and consequently viral parameters returned to pre-treatment levels over 18 weeks after siHBV was stopped in all mice (Figure 5*E*,*F*). In contrast, siHBV1 or siHBV2 pre-treatment followed by TherVacB resulted in a loss of serum HBsAg, HBeAg and HBV-DNA, development of high anti-HBs titers and anti-HBe seroconversion (Figure 5*E-I*), indicating a “cure” of HBV infection through induction of potent HBV-specific immunity.

Overall, the sequential treatment with siHBV1/2 and TherVacB was well tolerated, as neither caused significant liver damage nor affected body weight of mice and resulted in only moderate serum ALT elevation (≤100 U/l, i.e. max. 2.5-fold ULN) (Figure 5*J-L;* Supplementary Figure 5*E*). Slightly elevated sALT levels were observed over a period of three months before they normalized indicating that vaccine-induced, HBV-specific effector T cells targeted and eliminated HBV-infected hepatocytes over time. In three out of twelve mice that had received siHBV1 or siHBV2 before TherVacB, we observed a transient rebound of HBeAg with a concomitant decrease of anti-HBe when siRNA effects weaned (blowouts in Figure 5*F*,*H*; Supplementary Figure 5 showing individual mice). This, however, was rapidly contained most likely by vaccine-induced HBV-specific T cells.

TherVacB after siRNA treatment achieves long-lasting T cell responses that eliminate HBV.

Twenty-two weeks after the start of TherVacB, we detected HBV-specific T cells in livers and spleens of all vaccinated, AAV-HBV-infected mice. While HBV S_{190}-specific T cells were increased in the liver (Figure 6*A,B*) and in the periphery (Supplementary Figure 6; gating strategy shown in Supplementary Figure 7) in particular after siHBV2 pre-treatment and subsequent TherVacB, only a tendency was observed for core(C_{93})-specific T cells. However, also core-specific T cells showed a higher functionality and more T cells stained positive for IFN-γ, TNF and granzyme B upon *ex vivo* peptide re-stimulation (Figure 6*C*). In addition, we detected lower levels of co-inhibitory receptor PD1, but not TIM-3 (Figure 6*D-F*). As expected, siRNA pretreatment had no effect on the MVA-specific T-cell response (Supplementary Figure 6*D-G*). Interestingly, animals in which a transient HBeAg rebound was observed showed higher expression of PD1 and TIM3 and lower HBV-specific CD8 T-cell responses, correlating with decreased HBV control (Supplementary Figure 5).

The sequential siHBV and TherVacB treatment resulted in HBV control in the majority of animals, including suppression of HBV pregenomic RNA expression (Figure 7*A*), elimination of HBV core-expressing hepatocytes (Figure 7*B*,*C*) and elimination of HBV-DNA from the liver (Figure 7*D*). This demonstrates that the combination of siHBV with TherVacB is able to overcome HBV-specific immune tolerance and can achieve a cure of HBV infection in mice.

Discussion

Our study demonstrates that high level antigen expression is a most relevant factor causing HBV-specific immune tolerance and preventing successful therapeutic vaccination in mice. At HBsAg levels found in the majority of patients with chronic hepatitis B, i.e. between 1,000 to 10,000 IU/ml, the inhibition of HBV antigen expression in hepatocytes using long-lived, hepatocyte-targeted siRNAs enabled a therapeutic vaccine approach to elicit its full immunogenic capacity. Application of TherVacB alone in two preclinical mouse models of chronic HBV infection with corresponding viral antigen levels induced high-titer anti-HBs and detectable CD4 T cell responses but failed to induce HBV-specific CD8 T-cell immunity and thus did not achieve control over HBV infection. Reducing HBV-antigen expression first by HBV-specific RNAi, however, allowed TherVacB to overcome HBV-specific CD8 T-cell tolerance in the AAV-HBV model reflecting vertical and in HBV-transgenic mice reflecting horizontal transmission of HBV. This demonstrates that lowering high-level HBV antigen expression is a key factor in overcoming immune tolerance and achieving immune control of chronic HBV infection through therapeutic vaccination.

While the AAV-HBV model is currently the most suited model of persistent HBV infection[18] to investigate the effect of immunotherapies, it still has limitations. It uses fully immunocompetent mice in which the infection can be “cured”, but unlike in natural infections, HBV cannot spread. HBV is expressed from an episomal AAV-HBV transcription template, and even cccDNA-like molecules are formed in the nucleus of infected hepatocytes[21]. Its control, however, will very likely differ from that of cccDNA established after natural infection in human hepatoctyes[18]. In addition, the duration of antigen exposure in these models substantially differs from that in chronically infected patients, who often have been infected for decades. We cannot exclude that a longer antigen exposure might induce an even more profound HBV-specific immunotolerance which cannot be broken by reducing antigen levels and stimulation of HBV-specific B- and T-cell responses by therapeutic vaccination. The fact that we were also able to break immunotolerance in HBV-transgenic mice, which were exposed to HBV antigens since birth, supports the notion

that a substantial HBV-specific immunotolerance may be broken by the combination of siHBV and TherVacB. This, however, needs to be evaluated in clinical studies.

Activating the patient´s immune system to gain control over persistent HBV is the ultimate goal of an immune therapy for chronic hepatitis B, to which virus-specific CD8 T cells are contributing by either secreting antiviral cytokines or by killing infected hepatocytes[18, 22]. Several mechanisms, however, may prevent immune-mediated control of HBV: (i) HBV circumvents triggering innate immunity and inflammation[23-25] that is required by dendritic cells for antigen-presentation and appropriate activation of CD8 T cells[26]; (ii) local elimination by hepatic NK cells[27] or hepatocytes[28] results in scarcity of virus-specific CD8 T cells; (iii) regulatory cell populations act locally in the liver to curtail the function of virus-specific effector CD8 T cells[29]; and (iv) high-level viral antigens render virus-specific CD8 T cells dysfunctional[30, 31]. It has not been possible to ascertain which of these factors promoting HBV-specific immune tolerance is most decisive for the failure of therapeutic vaccination. In our study, failure of TherVacB to induce effective HBV-specific CD8 T-cell responses in high-titer mice correlated with high-level PD1 expression. In particular the mice in which HBeAg rebounded when siHBV effects had faded-out showed elevated PD1 levels. Using two different siRNAs, the slightly more effective one (siHBV2) resulted in a more pronounced reduction of PD1 and a complete loss of HBV. This indicated that PD1 overexpression in HBV-specific CD8 T cells may result from high hepatic HBV-antigen expression and be responsible for dysfunction of HBV-specific T-cell responses after TherVacB.

siRNAs constitute a very promising, potential therapeutic approach to limit HBV antigen expression in infected hepatocytes. Since all HBV RNAs terminate at the same polyadenylation site, an appropriately designed single siRNA is sufficient to target the 3' end of all HBV RNAs[14]. Systematic screening of target sites resulted in selection of siRNA candidates that successfully target the major HBV strains found world-wide. Coupling of these selected HBV-specific siRNAs to GalNAc for efficient delivery into hepatocytes[15] enhanced metabolic stability and resulted in long duration of action[32, 33], allowing for injection intervals to once every four weeks. Importantly,

neither reduction of HBV antigen levels by RNAi alone nor in combination with innate immune stimulation using a control vaccination scheme sufficed to break HBV-specific immune tolerance. This demonstrates that high-level HBV antigens do not simply actively suppress already existing HBV-specific immunity. It rather indicates that presentation of HBV antigens by dendritic cells in the context of an inflammatory microenvironment induced by therapeutic vaccination is required to newly prime protective HBV-specific T-cell immunity. We also show that controlling the virus load only with nucleoside analogues or capturing circulating HBV antigens by inducing anti-HBs antibodies[34] failed to enable therapeutic vaccination to control HBV. This strongly indicates that hepatocyte expression of viral antigens and MHC-restricted presentation of peptides derived from HBV antigens governs downregulation of HBV-specific CD8 T-cell immunity generated by therapeutic vaccination. The reduction of HBV antigen expression in hepatocytes followed by heterologous prime-boost therapeutic vaccination therefore function synergistically to achieve full immune control over HBV replication, reach a sustained reduction of HBsAg and HBeAg to undetectable levels, and finally eliminate HBV-positive hepatocytes from the livers of HBV carrier mice.

Elimination of HBV-infected hepatocytes following sequential therapy with siHBV and TherVacB was a process that occurred over weeks and was accompanied by low-grade hepatitis. This is consistent with vaccination-induced HBV-specific CD8 T cells gradually eliminating hepatocytes presenting HBV antigen-derived peptides on MHC class I molecules once RNAi suppression of HBV-antigen expression waned. Such sustained execution of antiviral immunity over prolonged periods of time may help to avoid overzealous immune pathology, and provides the basis for a potential immune therapy in patients with chronic hepatitis B. Particulate HBsAg and HBV core antigen and MVA-based vaccine vectors comparable to the components used in TherVacB[35], as well as GalNAc-coupled siRNAs[33] have already been applied safely to humans, suggesting that clinical translation of the approach presented is possible.

In conclusion, our study showed that high-level HBV-antigen expression causes HBV-specific immune tolerance in two relevant, preclinical models of persistent HBV infection. It provides preclinical proof-of-concept that a well-designed therapeutic hepatitis B vaccine has the potential to achieve immune control of HBV infection in the 25-30% patients with low HBsAg levels (HBsAg <1,000 IU/ml). In patients with higher antigen levels, however, a combination with siRNA pre-treatment may be required to enable therapeutic vaccination to control HBV. Therefore, a combination of siRNA and therapeutic vaccination represents a potential treatment option for the majority of chronically HBV-infected patients, and should be evaluated in clinical trials.

References and Notes

(Author names in bold designate shared co-first authorship)

1. Word Health Organisation W. Global Hepatitis Report 2017: Geneva: World Health Organisation, 2017.
2. Graber-Stiehl I. The silent epidemic killing more people than HIV, malaria or TB. Nature 2018;564:24-26.
3. Chen JD, Yang HI, Iloeje UH, et al. Carriers of inactive hepatitis B virus are still at risk for hepatocellular carcinoma and liver-related death. Gastroenterology 2010;138:1747-54.
4. Gehring AJ, Protzer U. Targeting Innate and Adaptive Immune Responses to Cure Chronic HBV Infection. Gastroenterology 2019;156:325-337.
5. **Lucifora J, Xia Y**, Reisinger F, et al. Specific and nonhepatotoxic degradation of nuclear hepatitis B virus cccDNA. Science 2014;343:1221-8.
6. Thimme R, Wieland S, Steiger C, et al. CD8(+) T cells mediate viral clearance and disease pathogenesis during acute hepatitis B virus infection. J Virol 2003;77:68-76.
7. Park JJ, Wong DK, Wahed AS, et al. Hepatitis B Virus--Specific and Global T-Cell Dysfunction in Chronic Hepatitis B. Gastroenterology 2016;150:684-695 e5.
8. Rehermann B. Pathogenesis of chronic viral hepatitis: differential roles of T cells and NK cells. Nat Med 2013;19:859-68.
9. Kosinska AD, Bauer T, Protzer U. Therapeutic vaccination for chronic hepatitis B. Curr Opin Virol 2017;23:75-81.
10. Michel ML, Bourgine M, Fontaine H, et al. Therapeutic vaccines in treating chronic hepatitis B: the end of the beginning or the beginning of the end? Med Microbiol Immunol 2015;204:121-9.
11. Backes S, Jager C, Dembek CJ, et al. Protein-prime/modified vaccinia virus Ankara vector-boost vaccination overcomes tolerance in high-antigenemic HBV-transgenic mice. Vaccine 2016;34:923-32.
12. Dumortier J, Schonig K, Oberwinkler H, et al. Liver-specific expression of interferon gamma following adenoviral gene transfer controls hepatitis B virus replication in mice. Gene Ther 2005;12:668-77.
13. Dion S, Bourgine M, Godon O, et al. Adeno-associated virus-mediated gene transfer leads to persistent hepatitis B virus replication in mice expressing HLA-A2 and HLA-DR1 molecules. J Virol 2013;87:5554-63.
14. Michler T, Grosse S, Mockenhaupt S, et al. Blocking sense-strand activity improves potency, safety and specificity of anti-hepatitis B virus short hairpin RNA. EMBO Mol Med 2016:10.15252/emmm.201506172.

15. Nair JK, Willoughby JL, Chan A, et al. Multivalent N-acetylgalactosamine-conjugated siRNA localizes in hepatocytes and elicits robust RNAi-mediated gene silencing. J Am Chem Soc 2014;136:16958-61.
16. Jeng WJ, Chen YC, Chien RN, et al. Incidence and predictors of hepatitis B surface antigen seroclearance after cessation of nucleos(t)ide analogue therapy in hepatitis B e antigen-negative chronic hepatitis B. Hepatology 2018;68:425-434.
17. Qiu YW, Huang LH, Yang WL, et al. Hepatitis B surface antigen quantification at hepatitis B e antigen seroconversion predicts virological relapse after the cessation of entecavir treatment in hepatitis B e antigen-positive patients. Int J Infect Dis 2016;43:43-48.
18. Guidotti LG, Ishikawa T, Hobbs MV, et al. Intracellular inactivation of the hepatitis B virus by cytotoxic T lymphocytes. Immunity 1996;4:25-36.
19. Protzer U. Viral hepatitis: The bumpy road to animal models for HBV infection. Nat Rev Gastroenterol Hepatol 2017;14:327-328.
20. Cheng L, Li F, Bility MT, et al. Modeling hepatitis B virus infection, immunopathology and therapy in mice. Antiviral Res 2015;121:1-8.
21. Lucifora J, Salvetti A, Marniquet X, et al. Detection of the hepatitis B virus (HBV) covalently-closed-circular DNA (cccDNA) in mice transduced with a recombinant AAV-HBV vector. Antiviral Res 2017;145:14-19.
22. **Xia Y**, **Stadler D**, Lucifora J, et al. Interferon-gamma and Tumor Necrosis Factor-alpha Produced by T Cells Reduce the HBV Persistence Form, cccDNA, Without Cytolysis. Gastroenterology 2016;150:194-205.
23. Wieland S, Thimme R, Purcell RH, et al. Genomic analysis of the host response to hepatitis B virus infection. Proc Natl Acad Sci U S A 2004;101:6669-74.
24. Hosel M, Quasdorff M, Wiegmann K, et al. Not interferon, but interleukin-6 controls early gene expression in hepatitis B virus infection. Hepatology 2009;50:1773-82.
25. Suslov A, Boldanova T, Wang X, et al. Hepatitis B Virus Does Not Interfere With Innate Immune Responses in the Human Liver. Gastroenterology 2018;154:1778-1790.
26. **Le Bon A**, **Etchart N**, Rossmann C, et al. Cross-priming of CD8+ T cells stimulated by virus-induced type I interferon. Nat Immunol 2003;4:1009-15.
27. Peppa D, Gill US, Reynolds G, et al. Up-regulation of a death receptor renders antiviral T cells susceptible to NK cell-mediated deletion. J Exp Med 2013;210:99-114.
28. Lopes AR, Kellam P, Das A, et al. Bim-mediated deletion of antigen-specific CD8 T cells in patients unable to control HBV infection. J Clin Invest 2008;118:1835-45.
29. Pallett LJ, Gill US, Quaglia A, et al. Metabolic regulation of hepatitis B immunopathology by myeloid-derived suppressor cells. Nat Med 2015;21:591-600.

30. Utzschneider DT, Legat A, Fuertes Marraco SA, et al. T cells maintain an exhausted phenotype after antigen withdrawal and population reexpansion. Nat Immunol 2013;14:603-10.
31. Utzschneider DT, Alfei F, Roelli P, et al. High antigen levels induce an exhausted phenotype in a chronic infection without impairing T cell expansion and survival. J Exp Med 2016;213:1819-34.
32. Foster DJ, Brown CR, Shaikh S, et al. Advanced siRNA Designs Further Improve In Vivo Performance of GalNAc-siRNA Conjugates. Mol Ther 2018;26:708-717.
33. Fitzgerald K, White S, Borodovsky A, et al. A Highly Durable RNAi Therapeutic Inhibitor of PCSK9. N Engl J Med 2017;376:41-51.
34. **Zhu D**, **Liu L**, Yang D, et al. Clearing Persistent Extracellular Antigen of Hepatitis B Virus: An Immunomodulatory Strategy To Reverse Tolerance for an Effective Therapeutic Vaccination. J Immunol 2016;196:3079-87.
35. Gilbert SC. Clinical development of Modified Vaccinia virus Ankara vaccines. Vaccine 2013;31:4241-6.

Acknowledgments: We thank Natalie Röder, Ruth Hillermann, Olga Seelbach, Daniela Heide and Judith Seebach for their excellent technical support and Dirk Busch for providing multimers.

Data and materials availability: All data is available in the main text or the supplementary materials. The TherVacB scheme is proprietary of the Helmholtz Zentrum Muenchen. c-di-AMP as an adjuvant is proprietary of the Helmholtz Center for Infection Research, Braunschweig, Germany. siHBV1/2 are proprietary of Alnylam Pharmaceuticals; rights have been licensed to VIR Biotechnology.

Figure Legends

Figure 1. HBV antigen titers determine the antiviral effect of therapeutic vaccination. (*A*) Distribution of serum HBsAg levels quantified in chronically HBV-infected patients in a clinical routine laboratory at the University Hospital rechts der Isar of Technical University of Munich. (*B-I*). High-viremic and -antigenemic, HBV-transgenic mice (n≥6/group; HBsAg 10^3 - 10^4 IU/ml; HBeAg >200 PEI U/ml) were transduced with a hepatotropic AAV vector expressing shRNA against HBV (shHBV) or a control shRNA (shCtrl). Eight weeks after shHBV, HBV-transgenic mice received a therapeutic hepatitis B vaccine (TherVacB; details see materials and methods). shRNA-treated control mice received adjuvant only and an MVA not expressing any transgene (ConVac) or no vaccine. Start of vaccination was week 0. (*B*,*C*) time kinetics, (*D*-*I*) endpoint analysis performed at day 7 after boost vaccination. Serum levels of (*B*) HBsAg, (*C*) HBeAg, (*D*) HBV-DNA and (*E*) anti-HBs antibodies. (*F*) Representative images of liver immunohistochemistry staining for HBV core (brown) and (*G*) quantification of cytoplasmic core-positive hepatocytes per mm^2. Scale bar 100 µm. (*H*) Southern blot analysis of pooled liver DNA per treatment group using an HBV-specific DNA probe. The HBV transgene (to control equal sample loading), relaxed circular and linear HBV genomes as well as HBV replication intermediates are indicated. Scans were cut at dotted lines to rearrange the order of groups. (*I*) Intrahepatic HBV-DNA levels of individual mice determined by quantitative PCR. Values corrected for the HBV transgene are given. (*B*,*C*) Mean±SEM is shown. (*D*,*E*,*G*,*I*) Values of individual mice are shown. Horizontal lines in (*D*,*E*) indicate mean and in (*G*,*I*) median values. Dotted lines indicate lower level of quantification (LLOQ) in (*D*) and sensitivity cut-off of the assay in (*E*). Statistical analysis was performed using (*B*,*C*) repeated measure 2-way Anova with Tukey´s multiple comparison correction, (*D*) Mann Whitney U test, (*E*,*G*) 1-way Anova with Sidak´s multiple comparison correction, or (*I*) Kruskal-Wallis with Dunn´s multiple comparison correction. Numbers in graphs indicate *p* values.

Figure 2. T-cell infiltration into the liver following therapeutic vaccination. High-viremic and -antigenemic, HBV-transgenic mice (see Figure 1) were transduced with an AAV expressing shHBV or a control shRNA (shCtrl). After 8 weeks mice received therapeutic vaccination and were sacrificed 7 days later. Representative pictures of liver sections stained with (*A*) haematoxylin-eosin (HE, upper row) or anti-CD3 (lower row), or (*B*) anti-CD4 or CD8 antibodies. Scale bars represent 100 µm, arrows mark exemplary positive cells and inlets show magnification of indicated areas. (*C*) Quantification of CD3-, CD4- and CD8-positive cells in liver sections of individual mice, horizontal lines indicate mean values. Statistical analysis was performed using 1-way Anova with Sidak´s multiple comparison correction, numbers in graphs indicate *p* values. (*D*) Histological scoring to assess liver pathology of individual mice.

Figure 3. Induction of HBV-specific CD8 T-cell responses by therapeutic vaccination after RNAi. High-viremic and -antigenemic, HBV-transgenic mice (see Figure 1) were transduced with an AAV expressing shHBV or a control shRNA (shCtrl). Eight weeks later, mice received therapeutic vaccination, and T-cell responses were analyzed 7 days thereafter by flow cytometry of intracellular cytokine staining following *ex vivo* peptide stimulation. To analyze CD8 T-cell responses, cells were stimulated with HBV peptides S_{208} or C_{93} or MVA peptide MVA_{B8R}. To analyze CD4 T-cell responses, cells were stimulated with overlapping HBV S- and core-specific peptide pools. (*A*) Exemplary flow cytometry of liver-associated CD8 T cells staining positive for IFN-γ (vertical) or TNF (horizontal). (*B-I*) Proportion of cells staining positive for indicated cytokines. Dots or triangles represent individual mice, horizontal lines indicate mean values. (*B*) MVA_{B8R}-reactive, IFN-γ_+ CD8 T cells isolated from liver (upper panel) or spleen (lower panel). (*C,D*) HBV-reactive CD4 (upper panel) or CD8 (lower panel) T cells isolated from (*C*) liver or (*D*) spleen. (*E-I*) Comparison of mice expressing either shCtrl (open triangles) or shHBV (filled dots) before TherVacB. Liver-associated CD8 T cells staining positive for indicated cytokines after stimulation with (*E*) S_{208}- or (*F*) C_{93}-peptide. Dots represent individual mice, horizontal lines indicate mean. (*G*) Correlation of serum ALT activity with HBV-specific (S_{208}-reactive) intrahepatic CD8 T cells. Correlation of frequencies of TherVacB-induced (*H*) S_{208}- or (*I*) C_{93}-reactive

intrahepatic CD8 T cells with serum HBsAg or HBeAg levels before vaccination. Statistical analysis was performed using (*B-D*) 1-way Anova with Sidak´s multiple comparison correction, (*E,F*) student T test and (*G-I*) two-tailed Pearson correlation. Numbers in flow cytometry blots indicate percentage of parental population and in diagrams *p* values.

Figure 4. Comparison of RNAi and antiviral treatment before therapeutic vaccination. High-antigenemic, HBV-transgenic mice (n≥6 / group) received four s.c. injections of GalNAc-coupled HBV-specific siRNAs, siHBV1 or siHBV2, or a control siRNA (siCtrl) every four weeks. Intravenous injection of AAV-shHBV or standard-of-care oral antiviral therapy with nucleoside analogue Entecavir (ETV) served as control. Twelve weeks after start of siHBV, shHBV or Entecavir treatment, TherVacB was initiated in all animals. Kinetics of (*A*) HBsAg and (*B*) HBeAg serum levels, mean±SEM is given. HBV viremia determined by quantitative PCR (*C*) before start of vaccination and (*D*) 7 days after boost vaccination. Dotted lines indicate lower level of quantification (LLOQ) of the assay. (*E-H*) Endpoint analyses performed at day 7 after boost vaccination. (*E*) Flow-cytometry analysis of intracellular cytokine staining of intrahepatic CD8 T cells after *ex vivo* stimulation with HBV-peptides $S_{208-215}$ (S_{208}) or $core_{93-100}$ (C_{93}). (*F*) Representative images of liver immunohistochemistry staining for HBV core protein (brown). Scale bars indicate 100 µm. (*G*) Quantification of cytoplasmic HBV core-positive hepatocytes. (*H*) HBV DNA levels determined in liver tissue lysates. (*C-E*,*G*,*H*) Values of individual mice are given, horizontal lines indicate median. Numbers in graphs indicate *p* values. Statistical analysis was performed using (*A*,*B*) 2-way repeated measure Anova with Dunnett´s multiple comparison correction, (*C*,*H*) Kruskal-Wallis test with Dunn´s multiple comparison correction or (*E*,*G*) 1-way Anova with Sidak´s multiple comparison correction.

Figure 5. Sustained control of HBV in AAV-HBV infected mice. (*A-D*) C57BL/6J mice were intravenously injected with indicated doses of an AAV vector carrying a 1.2-fold overlength HBV genome (AAV-HBV) to establish different levels of HBV replication. Vaccination with TherVacB

was started 4 weeks after AAV-HBV infection. Kinetics of (*A*) HBsAg and (*B*) HBeAg serum levels; mean ± SEM per group (n=4) is shown. At week 5 after start of TherVacB, animals were sacrificed and analyzed. (*C*) Serum anti-HBs titers. (*D*) HBV-specific, liver-associated CD8 T cells detected by flow cytometry after intracellular cytokine staining following *ex vivo* stimulation with HBV-derived peptide core$_{93\text{-}100}$ (C_{93}). (*C,D*) Diamonds represent individual mice, horizontal lines indicate mean.

(*E-L*) Persistent, high-titer HBV replication was established in a new set of C57BL/6 mice (n≥6 / group) by intravenous injection of the second highest dose of AAV-HBV. After 4, 8 and 12 weeks, GalNAc-coupled siHBV1, siHBV2 or siCtrl were injected s.c.. Together with the last siRNA dose, TherVacB was initiated (week 0). Mice receiving no vaccination served as controls. (*E-H*) Kinetics of (*E*) HBsAg, (*F*) HBeAg, (*G*) anti-HBs, (*H*) anti-HBe serum levels; mean ± SEM is shown. Blowouts show HBeAg (upper panel) and anti-HBe (lower panel) serum levels detected for individual mice with HBeAg rebound (colored lines indicate identical animals). (*I*) Serum HBV-DNA determined at sacrifice (week 22). (*J*) Body weight determined at indicated time points. (*K*) Median ALT activity in serum / group. (*L*) Histological scoring to assess liver pathology of individual mice. Dotted lines indicate sensitivity cut-off of the assay in (*A,B,C,E,G,H*) and lower level of quantification (LLOQ) in (*I*). Statistical analysis was performed using (*G*,*F*,*K*) 2-way repeated measure Anova with Dunnett´s or 1-way Anova with (*C,D*) Dunnett´s or (*I*) Sidak´s multiple comparison correction. Numbers in graphs indicate *p* values. n.d.: not determined.

Figure 6. Induction of long-lasting, polyfunctional and polyspecific T-cell responses. Identical experimental groups as in Fig. 5 *E-M*. Persistent, high-titer HBV replication (HBsAg 10^3-10^4 IU/ml) was established in C57BL/6 mice by infection with AAV-HBV. GalNAc-coupled siHBV1, siHBV2 or siCtrl were injected s.c. 4, 8 and 12 weeks after AAV-HBV. Together with the last siRNA dose, TherVacB was initiated (week 0). Endpoint analysis was at week 22. Mice receiving no vaccination served as controls (*A,B*) Liver-associated T cells were stained directly *ex vivo* using S208-215 (S_{208}) and core93-100 (C_{93}) multimers. (*A*) Exemplary flow-cytometry results. (*B*) For each animal the fraction of multimer-positive CD8 T cells is given. (*C*) Fraction of intrahepatic

CD8 T cells staining positive for indicated cytokines after *ex vivo* stimulation with S- (upper panel) or core- (lower panel) specific overlapping peptide pools. (*D,E*) Surface staining of intrahepatic, C_{93}-multimer positive CD8 T cells for PD1 and Tim3. (*D*) Exemplary flow cytometry results with gating on total $PD1^{+}$ (thin line) or $PD1^{high}$ (bold line) fractions. (*E*) Quantification of $PD1^{high}$ and/or $TIM3^{+}$ C_{93}-specific CD8 T cells (left panel) and mean fluorescence intensity (MFI) of PD1 staining (right panel). (*F*) Correlation of PD1 expression levels on C_{93}-$multimer^{+}$ CD8 T cells with cytokine production following *ex vivo* stimulation with a core-specific peptide pool. In (*B,C,E,F*), values of individual mice are shown, horizontal lines indicate median. Statistical analysis was performed using Kruskal-Wallis test with Dunn´s multiple comparison correction. Numbers in flow cytometry blots indicate percentage of parental population, numbers in diagrams show *p* values.

Figure 7. A combination of siRNA and TherVacB eliminates HBV. Experimental set-up as in Figure 5*E-M* and 6. Endpoint analysis was performed 22 weeks after the start of TherVacB. (*A*) Levels of 3.5 kb HBV-RNA (indicated as pregenomic HBV RNA) were quantified in livers lysates by PCR. (*B*) Representative images of liver immunohistochemistry staining for HBV core protein (brown). (*C*) Quantification of hepatocytes with core-positive nuclei. Mean numbers per mm^2 within three tissue areas of at least 10 mm^2 are given. Scale bars indicate 100 µm. (*D*) Intrahepatic HBV-DNA levels quantified by PCR. Values corrected for the AAV-HBV DNA template are given. In (*A,C,D*), values of individual mice are shown, with horizontal lines indicating median. Statistical analysis was performed using Kruskal-Wallis test with Dunn´s multiple comparison correction. Numbers in graphs indicate *p* values.

Supplementary material for manuscript:

RNA interference enables therapeutic vaccination to control and eliminate hepatitis B virus in high-titer carrier mice

Short title: RNAi enables therapeutic hepatitis B vaccination

Authors

Thomas Michler[1,10] *, Anna D. Kosinska[1,10] *, Julia Festag[1], Till Bunse[1,10], Jinpeng Su[1], Marc Ringelhan[1,2], Hortenzia Imhof[1], Dirk Grimm[3,10], Katja Steiger[4], Carolin Mogler[4], Mathias Heikenwalder[5], Marie-Louise Michel[6], Carlos A. Guzman[7,10], Stuart Milstein[8], Laura Sepp-Lorenzino[8], Percy Knolle[9,10], Ulrike Protzer[1,10]

* the authors contributed equally to the work

Affiliations

[1]Institute of Virology, Technical University of Munich / Helmholtz Zentrum München, Trogerstrasse 30, D-81675 Munich, Germany.

[2]Department of Internal Medicine II, University Hospital rechts der Isar, Technical University of Munich, Ismaninger Str. 22, D-81675 Munich, Germany.

[3]Department of Infectious Diseases/Virology, Heidelberg University Hospital, BioQuant, Im Neuenheimer Feld 267, D-69120 Heidelberg, Germany.

[4]Institute of Pathology, Technical University of Munich, Trogerstrasse 18, D-81675 Munich, Germany.

[5]Division of Chronic Inflammation and Cancer, German Cancer Research Center (DKFZ), Im Neuenheimer Feld 242, D-69120 Heidelberg, Germany.

[6]Institut Pasteur, 28 rue Dr Roux, 75015 Paris, France.

[7]Department of Vaccinology and Applied Microbiology, Helmholtz Centre for Infection Research, Inhoffenstr. 7, D-38124 Braunschweig, Germany.

[8]Alnylam Pharmaceuticals, 300 Third Street, Cambridge, MA 02142, USA.

[9]Institute of Molecular Immunology, University Hospital rechts der Isar, Technical University of Munich, Ismaninger Strasse 22, D-81675 Munich, Germany.

[10]German Center for Infection Research (DZIF), Munich, Heidelberg and Hannover/Braunschweig partner sites, Germany.

Supplementary Materials and Methods

Therapeutic hepatitis B vaccine (TherVacB). Mice were immunized with a heterologous protein-prime / recombinant Modified Vaccinia Ankara virus (MVA) vector-boost vaccination scheme, as described[11]. Briefly, mice were immunized intramuscularly (i.m.) twice with 15 µg of particulate HBsAg (genotype A, adw) expressed in yeast and 15 µg of HBV core protein (genotype D, ayw) particles purified from *E. coli* (kindly provided by APP Latvijas Biomedicinas, Riga, Latvia) adjuvanted with 10 µg cyclic di-adenylate monophosphate (c-di-AMP) (InvivoGen, San Diego, CA, USA). Two weeks after the second protein vaccination, mice were boosted by i.m. injection of $5x10^7$ plaque-forming units (PFU) each of recombinant MVA vectors expressing HBV S or HBV core protein (both genotype D, ayw). Control vaccination consisted of two i.m. injections of the adjuvants without HBV proteins and a boost with an MVA not expressing any transgene. Mice were sacrificed one week (HBVtg mice) or 18 weeks (long-term efficacy study in AAV-HBV model) after MVA boost immunization. Blood and organs were collected for further analysis.

Serological analyses. Serum HBsAg, HBeAg and anti-HBs levels were quantified on an Architect™ platform after dilution with the Architect HBsAg Manual Diluent (lowest dilution 1:5) using the quantitative HBsAg test (Ref.: 6C36-44; Cutoff: 0.25 IU/ml), the HBeAg Reagent Kit (Ref.: 6C32-27) with HBeAg Quantitative Calibrators (Ref.: 7P24-01; Cutoff: 0.20 PEI U/ml) and the anti-HBs test (Ref.: 7C18-27; Cutoff: 12.5 mIU/ml) (all Abbott Laboratories, Wiesbaden, Germany), respectively. Anti-HBe levels were determined after 1:6 dilution in phosphate-buffered saline (PBS) plus 10% fetal calf serum (FCS) using the Enzygnost™ anti-HBe monoclonal test (data given in Relative Light Units [RLU] with >0.832 RLU considered negative) on the BEPIII platform (Siemens Healthcare, Eschborn, Germany). Serum alanine aminotransferase (ALT) activity was measured in a 1:4 dilution in PBS using the Reflotron® GPT/ALT test (Roche Diagnostics, Mannheim, Germany). Values and cutoffs of quantitative tests are given after correction for the respective dilution.

Analysis of HBV DNA in serum and liver. DNA was extracted from 25 µl of serum using the QIAamp MinElute Virus Spin Kit (Qiagen, Hilden, Germany) according to the manufacturer's protocol and eluted into 50 µl H_2O. For qPCR analysis from liver tissue, DNA was extracted using the NucleoSpin Tissue kit (Macherey-Nagel, Düren, Germany). Quantitative HBV-specific real-time PCR (lower limit of quantification [LLOQ]: 1.705 copies / µl serum) was performed on an Applied Biosystems® 7500 Real-time PCR system (Thermo Fisher Scientific, Darmstadt, Germany) using primers HBV1464_fw / HBV1599_rev and a Taqman probe. To determine HBV genome copy numbers per cell in the transgenic mouse model, numbers of diploid cell genomes were subtracted as the HBV-specific PCR also amplifies the HBV integrate. Values determined for HBV genome copy numbers per cell in the AAV-HBV model were corrected for the AAV-HBV by subtracting AAV-copies using AAV_ITR primers. Cell numbers were determined by real-time PCR for the single-copy mouse prion protein gene (mPrp). For primer/probe sequences and cycling conditions, see Supplementary Table 1. For Southern blot analysis, frozen liver samples were lysed using the Tissue Lyser LT (Qiagen), and after adding 20% SDS and digestion with proteinase K and RNase A, DNA was extracted with phenol-chloroform. Equal amounts of DNA extracted from individual animals within the same treatment group were pooled, digested overnight with *Hind III* (Thermo Fisher Scientific), separated through a 1.0% agarose gel, transferred onto a nylon membrane and UV cross-linked prior to overnight hybridization with a digoxigenin-labeled DNA probe at 65°C. HBV-DNA was visualized using the DIG Luminescent Detection kit (Roche Diagnostics) on an ECL Chemocam (INTAS Science Imaging Instruments, Göttingen, Germany).

Analysis of HBV transcripts. RNA was extracted from livers using the RNeasy Mini kit (Qiagen). cDNA was reverse transcribed using the SuperScript III kit (Thermo Fisher Scientific) and HBV transcripts were amplified by real-time RT-PCR on a LightCycler® 480 Instrument II (Roche Diagnostics) with primers to detect only HBV 3.5 kb transcripts that mainly consist of HBV pregenomic RNA. Results were normccccvalized to expression of Glyceraldehyde 3-phosphat

dehydrogenase (GAPDH). For primer sequences and cycling conditions, see Supplementary Table 1.

Histology and immunohistochemistry. Livers were fixed in 4% buffered formalin for 48 h, dehydrated and embedded in paraffin before serial 2 µm-thin sections were prepared. Hematoxylin-Eosin (HE) staining was performed on deparaffinized sections with Eosin and Mayer´s Haemalaun according to standard protocols. Histopathological evaluation was performed by an experienced liver pathologist in a blinded manner. A general description of histopathological findings was provided as well as a grading system including severity of inflammation, necrosis and fibrosis ranging from 0 (=none) to 3 (=very strong). For immunohistochemistry, rabbit anti-CD3 (Zytomed Systems GmbH, Berlin, Germany; #RBK024-05; 1:250 dilution; retrieval at 95°C for 30 min with EDTA), rat anti-CD4 (eBioscience, Frankfurt a. Main, Germany; #14-9766-82; 1:1,000 dilution; retrieval at 100°C for 30 min with EDTA) or rabbit anti-HBV core (Diagnostic Biosystems, Pleasanton, CA, USA; #RP 017; 1:50 dilution; retrieval at 100°C for 30 min with EDTA) were used on a Leica Bond MAX system (Leica Biosystems, Nussloch, Germany). Anti-CD8 stains were performed on cryo-conserved tissue using rat primary anti-CD8 (BD Bioscience; #553027; 1:200 dilution). For analysis, tissue slides were scanned using a SCN 400 slide scanner (Leica Biosystems). Positive cells were quantified from at least three tissue areas adding up to ≥10 mm^2 using the integrated Tissue AI software (Leica Biosystems).

Supplementary figure legends and table

Supplementary Figure 1. Effects of therapeutic hepatitis B vaccine TherVacB in high-viremic and -antigenemic HBV-transgenic mice. High-viremic and -antigenemic HBV-transgenic mice (n≥6/group) received therapeutic hepatitis B vaccine TherVacB at week 0. Control mice received adjuvant only and a MVA vector not expressing any transgene (ConVac) or no vaccine. Endpoint analysis was performed at day 7 after boost vaccination. (*A*-*C*) Kinetics of the effect of TherVacB on serum (*A*) HBsAg, (*B*) HBeAg and (*C*) HBV-DNA levels. (*D*) Serum anti-HBs and (*E*) anti-HBe levels at the endpoint. (*A*-*C*) Mean±SEM is shown. (*D*,*E*) Values of individual mice are shown, bars indicate mean values. (*D,E*) Negative values are displayed below cutoff line. Statistical analysis was performed using (*A*) 2-way repeated measured Anova with Sidak´s multiple comparison correction and (*C*) 1-way Anova with Dunnett´s multiple comparison correction. Numbers in graphs indicate *p* values.

Supplementary Figure 2. Effects of shRNA pre-treatment and therapeutic hepatitis B vaccine TherVacB. High-viremic and -antigenemic HBV-transgenic mice (n≥6/group; HBsAg 10^3 - 10^4 IU/ml; HBeAg >200 PEI U/ml) were transduced with a hepatotropic AAV vector expressing shRNA against HBV (shHBV) or a control shRNA (shCtrl). Eight weeks after AAV transduction, vaccination with TherVacB was started. Control mice received no vaccine. (*A*) Kinetics of serum ALT activity. (*B*) Endpoint analysis was performed at day 7 after boost vaccination. Representative photographs of CD4 and CD8 stainings of liver sections. Scale bars indicate 100 µm, arrows positive cells. In (*A*) Mean±SEM is shown. Statistical analysis was performed using 1-way Anova with Dunnett´s multiple comparison.

Supplementary Figure 3. Effect of vaccination on HBV-specific T-cell response. High-viremic and -antigenemic HBV-transgenic mice (n≥6/group; HBsAg 10^3 - 10^4 IU/ml; HBeAg >200 PEI U/ml) were treated with TherVacB, a control vaccine consisting of adjuvant only and a MVA vector not expressing any transgene (ConVac), or no vaccine. Seven days after boost vaccination, T

cells were isolated from liver and stimulated *ex vivo* with HBV- or MVA-derived peptides and analyzed via intracellular cytokine staining. (*A*) Results of animals which only received vaccination but were not treated with an AAV-shRNA vector. (upper panels) CD4 T cells staining positive for TNF or IFN-γ after stimulation with overlapping HBV S- and core-specific peptide pools. (lower panels) CD8 T cells staining positive for IFN-γ after stimulation with HBV peptides S_{208}-and C_{93}. (*B*) CD8 T-cell responses of animals which were treated with an AAV-shRNA vector and ConVac in liver (upper panels) or spleen (lower panels) determined after *ex vivo* stimulation with HBV-specific (S_{208} and C_{93}) or MVA-specific (B8R) peptides. Values of individual mice are shown, bars indicate mean values. Statistical analysis was performed using 1-way Anova with Sidak´s multiple comparison correction. Numbers in graphs indicate *p* values.

Supplementary Figure 4. Effect of RNAi or Entecavir pre-treatment and TherVacB vaccination. High-antigenemic HBV-transgenic mice (n≥6/group) were pretreated with four subcutaneous injections of GalNAc-coupled HBV-specific siRNAs (siHBV1/siHBV2) or a control siRNA (siCtrl) every four weeks. Intravenous injection of an AAV vector expressing shHBV, or standard-of-care oral antiviral therapy with nucleoside analogue Entecavir (ETV) were additional controls. Twelve weeks after the start of HBV siRNA/shRNA or Entecavir, TherVacB was initiated in all animals. Endpoint analysis was performed 7 days after boost vaccination. (*A*) Serum anti-HBs levels, (*B*) intrahepatic CD8 T cell numbers determined by immunohistochemistry staining of liver sections and (*C*) MVA_{B8R}-reactive intrahepatic CD8 T cells detected by intracellular cytokine staining after *ex vivo* peptide stimulation. (*D*) Histological scoring to assess pathologic changes in liver tissue. Score of 0 represents no changes, score of 3 distinct alterations. (*A*-*D*) Values of individual mice are shown, bars indicate (*A*-*C*) mean or (*D*) median values. Statistical analysis was performed using 1-way Anova with Sidak´s multiple comparison correction. Numbers in graphs indicate *p* values.

Supplementary Figure 5. Analysis of individual mice receiving HBV siRNA and TherVacB: HBeAg rebounder versus controller. Results of individual, AAV-HBV-transduced mice which

received GalNAc-coupled siHBV1 or siHBV2 followed by TherVacB are shown (grouped analysis of the different treatment groups is shown in Figure 5*E-M* and Figures 6,7). Animal showing an HBeAg rebound are highlighted in color in all graphs. (*A-D*) Kinetics of serum levels of (*A*) HBsAg, (*B*) HBeAg, (*C*) anti-HBs and (*D*) anti-HBe. n.d.: not determined. (*E*) Serum ALT activity started at week 4, when MVA-boost vaccination was applied. (*F-I*) Endpoint analysis was performed 22 weeks after the start of TherVacB. (*F*) Intracellular cytokine staining (IFN-γ upper row; TNF lower row) of intrahepatic CD8 T cells after *ex vivo* stimulation with HBV S- or core-specific overlapping peptide pools. (*G*) Flow cytometry analysis of intrahepatic T cells staining positive for PD1- and/or Tim3, gated on C_{93}-multimer-positive CD8 T cells. For gating on total PD1 positive or $PD1_{high}$ fractions see Figure 6*D*. MFI, Mean fluorescence intensity. (*H*) Levels of 3.5 kb HBV-RNA (including pregenomic RNA) were determined in liver lysates by real time (RT-)PCR and normalized to GAPDH. (*I*) Quantification of hepatocytes expressing core in nucleus as determined by immunohistochemistry stainings. Bars indicate (*F,H,I*) median or (*G*) mean values. (*A,C,D,I*) Negative values are displayed below cutoff line. Statistical analysis was performed with Kruskal-Wallis test with Dunn´s multiple comparison correction. Numbers in graphs indicate *p* values**.**

Supplementary Figure 6. Combination of HBV siRNA and TherVacB induces HBV-specific T-cell responses in AAV-HBV mouse model. Persistent, high-titer HBV replication (HBsAg 10^3 - 10^4 IU/ml; HBeAg >100 PEI U/ml) was established in C57BL/6 mice (n≥6/group) by intravenous injection of $2x10^{10}$ genome equivalents of an AAV vector carrying a 1.2-fold overlength HBV genome (AAV-HBV). Starting at 4 weeks after AAV-HBV transduction, HBV-specific GalNAc-coupled siHBV1, siHBV2 or siCtrl were injected subcutaneously three times every four weeks. Together with the last siRNA dose, TherVacB was initiated. Mice receiving no vaccination served as controls. Endpoint analysis was performed 22 weeks after the start of TherVacB. (*A-C*) Absolute numbers of CD8 T cells in (*A*) liver or (*B*) spleen or of (*C*) HBV-specific CD8 T cells in liver (left graph, S_{190}-multimer$_+$; right graph, C_{93}-multimer$_+$) were determined by flow cytometry using counting beads. (*D,E*) T cells isolated from liver were *ex vivo* stimulated with overlapping HBV S- and core-specific peptide pools or MVA_{B8R} and cytokine production measured by

intracellular staining. (*D*) Exemplary flow-cytometry results. (*E*) Quantification of CD8 T cells staining positive for IFN-γ. (*F*) HBV S_{190}-, C_{93}- and MVA_{B8R}-specific CD8 T cells in spleen were determined by multimer staining directly *ex vivo* and (*G*) cytokine production (IFN-γ upper row; TNF lower row) after *ex vivo* stimulation with the respective peptide was measured by intracellular cytokine staining. (*A*-*G*) Values of individual mice are shown, bars indicate mean values. Statistical analysis was performed with Kruskal-Wallis test with Dunn´s multiple comparison correction. Numbers in flow cytometry blots indicate percentage of parental population and in diagrams *p* values.

Supplementary Figure 7. Gating strategy of flow cytometric analysis. (*A*) Lymphocyte population was defined using forward-scattered-light-height (FSC-H) and side-scattered-light-height (SSC-H) parameters (left diagram). Doublets were excluded from lymphocyte population by plotting forward-scattered-light height (FSC-H) against area (FSC-A) and gating on the diagonal population (middle diagram). Dead cells were excluded from analysis by gating on fixable viability dye (FVD-eFluor780-A)-negative cells (right diagram). (*B*) CD4 or CD8 T cells were gated within the viable lymphocyte population using CD4 APC-A and CD8 PB450-A for intracellular cytokine staining (ICS), and CD8 KO525-A for multimer staining. (*C*) To determine IFN-γ+, TNF+ single- or double-positive cells via ICS, populations of CD4 or CD8 T cells were plotted using IFN-γ-FITC-A against TNF-PE-Cy7-A. (*D*,*E*) IFN-γ+ or multimer+ CD8 T cells were evaluated by plotting (*D*) IFN-γ-FITC-A or (*E*) multimer-PE-A against CD8. Positioning of gates was determined using controls stimulated with ovalbumin-derived peptide $S8L_{257-264}$ (OVA_{S8L}; SIINFEKL) for ICS or staining with OVA_{S8L}-conjugated MHC class I multimers. H = height; A = area; APC = Allophycocyanin; PB450 = Pacific Blue™ 450; FITC = Fluorescein isothiocyanate; PE-Cy7 = Phycoerythrin-Cyanin 7; PE = Phycoerythrin.

Supplementary Table 1: Oligonucleotides and cycling conditions used for PCR

Oligonucleotide	Target	Sequence (5' to 3')
HBV1464_fw*	HBV DNA	GGACCCCTTCTCGTGTTACA
HBV1599_rev*	HBV DNA	ACTGCGAATTTTGGCCAAGA
HBV1529_probe*	HBV DNA	FAM-TCTAGACTCGTGGTGGACTTCTCTCAATTTTCT-TAMRA**
Cycling conditions: 2 min 50°C, 10 min 95°C followed by 45× (15 s 95°C, 1 min 60°C)		
mPrp_fw	murine *prp* gene	GCGGTACATGTTTTCACGGTAGTA
mPrp_rev	murine *prp* gene	GAGCAGGCCCATGATCCA
mPRP_probe	murine *prp* gene	VIC-CGGTCCTCCCAGTCGTTGCCAAAA-TAMRA**
Cycling conditions: 2 min 50°C, 10 min 95°C followed by 45× (15 s 95°C, 1 min 60°C)		
AAV_ITR_fw	AAV ITR	AACCCGCCATGCTACTTATCTACCT
AAV_ITR_rev	AAV ITR	CAAACAGTCTTTGAAGTATGCC
Cycling conditions: 5 min 95°C followed by 40× (15 s 95°C, 10 s 60°C, 25 s 72°C)		
HBV3.5kbRNA_fw	HBV 3.5 kb RNA	GAGTGTGGATTCGCACTCC
HBV3.5kbRNA_rev	HBV 3.5 kb RNA	GAGGCGAGGGAGTTCTTCT
Cycling conditions: 5 min 95°C followed by 40× (3 s 95°C, 30 s 60°C)		
mGAPDH_fw	murine *gapdh* gene	ACCAACTGCTTAGCCC
mGAPDH_rev	murine *gapdh* gene	CCACGACGGACACATT
Cycling conditions: 5 min 95°C followed by 40× (15 s 95°C, 10 s 60°C, 25 s 72°C)		

*numbering of HBV primers refers to the 5' nucleotide with the A in core ATG set to 1.

**FAM = 6-Carboxyfluorescein; TAMRA= Tetramethylrhodamine; VIC= 4,7,2`trichloro-7`phenyl-6-carboxyfluorescein.

Figure 1

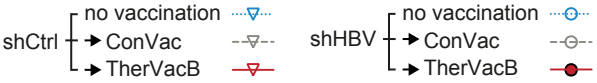
shCtrl
no vaccination
ConVac
TherVacB
shHBV
no vaccination
ConVac
TherVacB

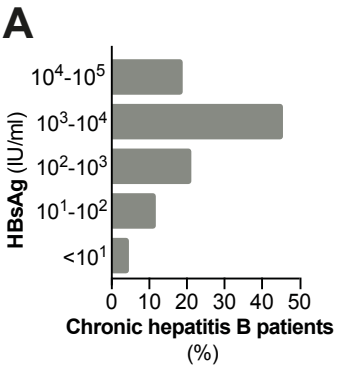
A
HBsAg (IU/ml)
10^4-10^5
10^3-10^4
10^2-10^3
10^1-10^2
<10^1
0 10 20 30 40 50
Chronic hepatitis B patients
(%)

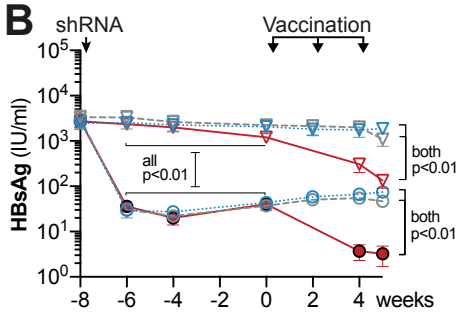
B
shRNA
Vaccination
HBsAg (IU/ml)
all
p<0.01
both
p<0.01
both
p<0.01
-8 -6 -4 -2 0 2 4 weeks

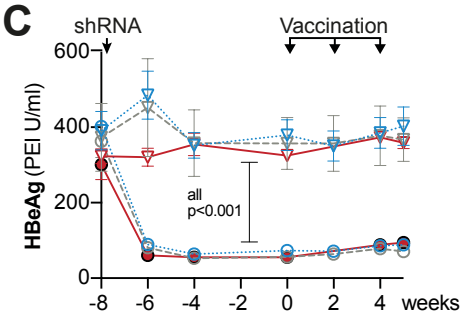
C
shRNA
Vaccination
HBeAg (PEI U/ml)
all
p<0.001
-8 -6 -4 -2 0 2 4 weeks

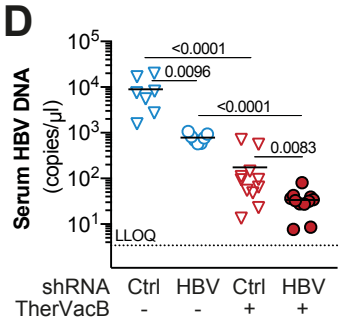
D
Serum HBV DNA
(copies/µl)
<0.0001
0.0096
<0.0001
0.0083
LLOQ
shRNA Ctrl HBV Ctrl HBV
TherVacB - - + +

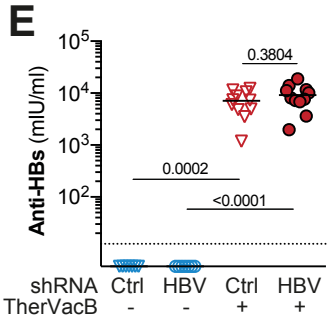
E
Anti-HBs (mIU/ml)
0.3804
0.0002
<0.0001
shRNA Ctrl HBV Ctrl HBV
TherVacB - - + +

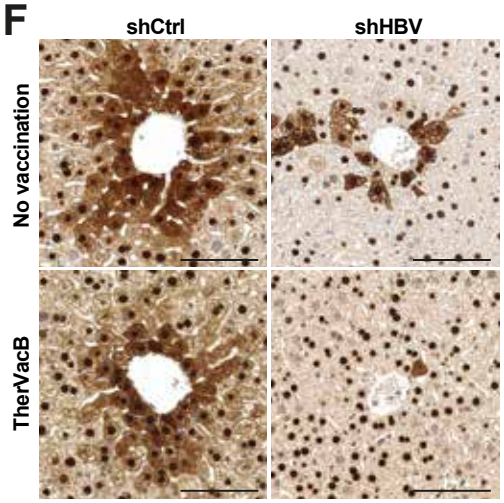
F
shCtrl
shHBV
No vaccination
TherVacB

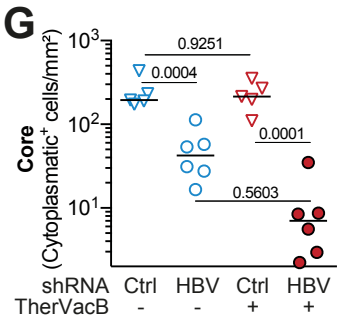
G
Core
(Cytoplasmatic+ cells/mm²)
0.9251
0.0004
0.0001
0.5603
shRNA Ctrl HBV Ctrl HBV
TherVacB - - + +

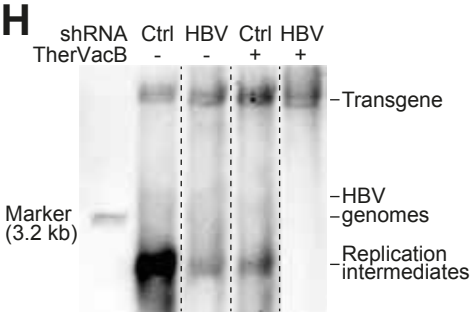
H
shRNA Ctrl HBV Ctrl HBV
TherVacB - - + +
Transgene
HBV
genomes
Replication
intermediates
Marker
(3.2 kb)

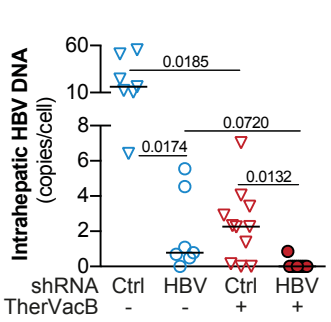
I
Intrahepatic HBV DNA
(copies/cell)
0.0185
0.0720
0.0174
0.0132
shRNA Ctrl HBV Ctrl HBV
TherVacB - - + +

Figure 2

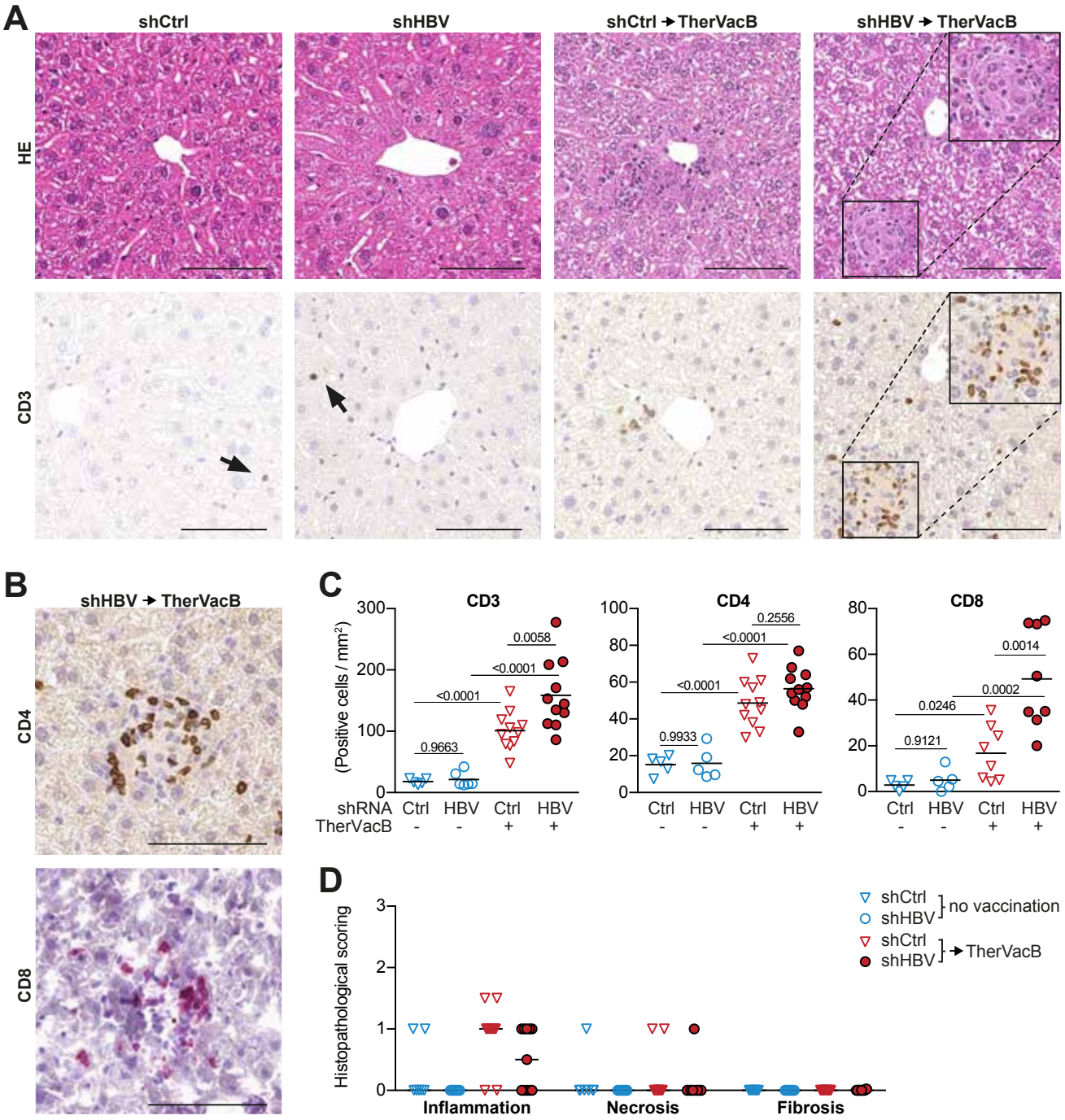
A
shCtrl
shHBV
shCtrl → TherVacB
shHBV → TherVacB
HE
CD3
B
shHBV → TherVacB
CD4
CD8
C
CD3
CD4
CD8
(Positive cells / mm²)
shRNA
TherVacB
Ctrl
HBV
0.9663
<0.0001
<0.0001
0.0058
0.9933
<0.0001
<0.0001
0.2556
0.9121
0.0246
0.0002
0.0014
D
Histopathological scoring
Inflammation
Necrosis
Fibrosis
shCtrl
shHBV
no vaccination
shCtrl
shHBV
→ TherVacB

Figure 3

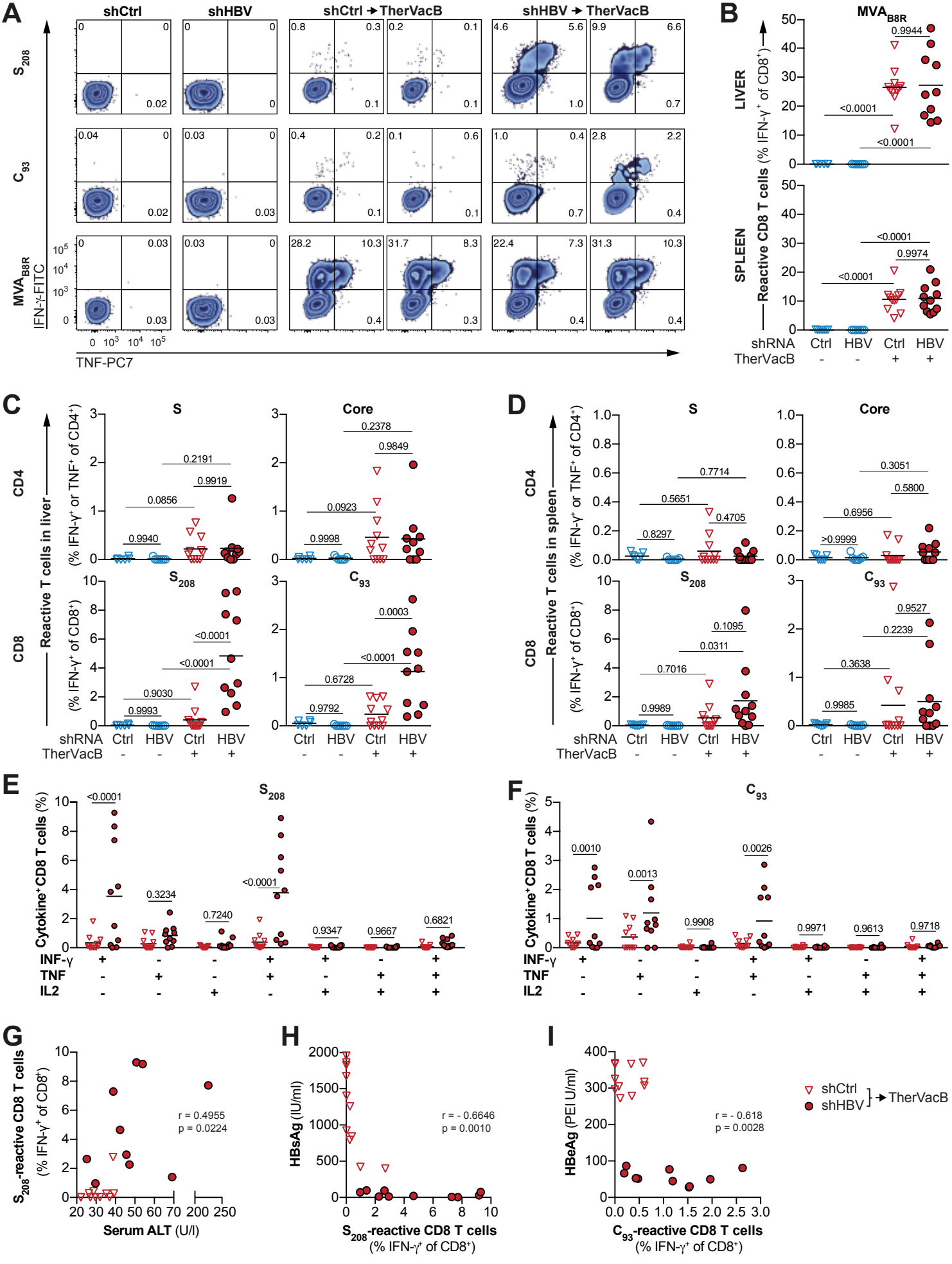
A
shCtrl
shHBV
shCtrl → TherVacB
shHBV → TherVacB
S208
C93
MVAB8R
IFN-γ-FITC
TNF-PC7
B
MVAB8R
LIVER
SPLEEN
Reactive CD8 T cells (% IFN-γ+ of CD8+)
shRNA Ctrl HBV Ctrl HBV
TherVacB - - + +
C
D
CD4
CD8
Reactive T cells in liver
Reactive T cells in spleen
S
Core
S208
C93
(% IFN-γ+ or TNF+ of CD4+)
(% IFN-γ+ of CD8+)
E
F
Cytokine+ CD8 T cells (%)
INF-γ
TNF
IL2
G
H
I
S208-reactive CD8 T cells (% IFN-γ+ of CD8+)
Serum ALT (U/l)
r = 0.4955
p = 0.0224
HBsAg (IU/ml)
S208-reactive CD8 T cells (% IFN-γ+ of CD8+)
r = - 0.6646
p = 0.0010
HBeAg (PEI U/ml)
C93-reactive CD8 T cells (% IFN-γ+ of CD8+)
r = - 0.618
p = 0.0028
shCtrl
shHBV
TherVacB

Figure 4

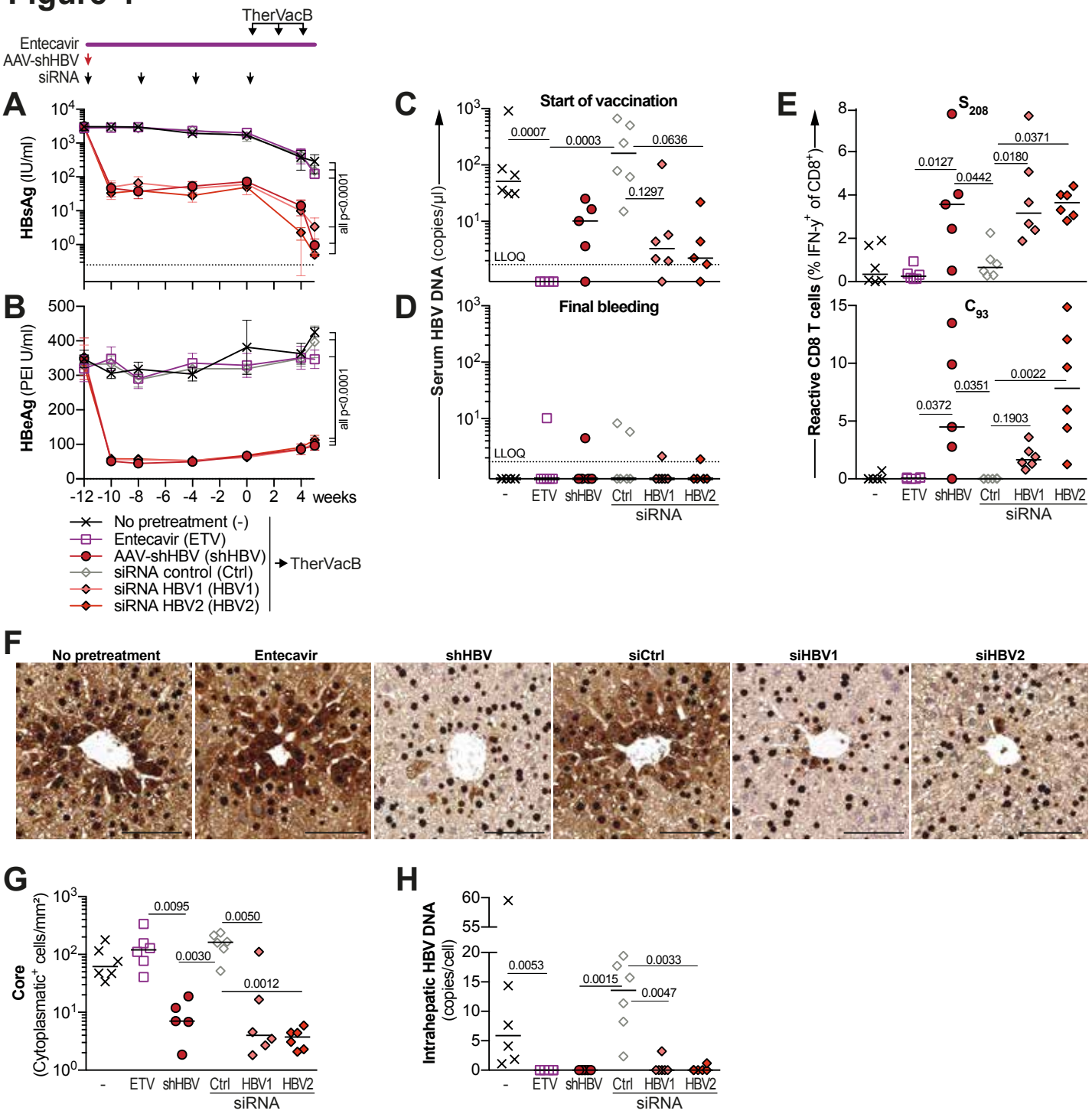
TherVacB
Entecavir
AAV-shHBV
siRNA
A
HBsAg (IU/ml)
all p<0.0001
B
HBeAg (PEI U/ml)
all p<0.0001
-12 -10 -8 -6 -4 -2 0 2 4 weeks
No pretreatment (-)
Entecavir (ETV)
AAV-shHBV (shHBV)
siRNA control (Ctrl)
siRNA HBV1 (HBV1)
siRNA HBV2 (HBV2)
TherVacB
C
Start of vaccination
Serum HBV DNA (copies/µl)
0.0007
0.0003
0.0636
0.1297
LLOQ
D
Final bleeding
LLOQ
- ETV shHBV Ctrl HBV1 HBV2
siRNA
E
S208
0.0127
0.0442
0.0371
0.0180
C93
0.0372
0.0351
0.1903
0.0022
Reactive CD8 T cells (% IFN-γ+ of CD8+)
- ETV shHBV Ctrl HBV1 HBV2
siRNA

F

No pretreatment
Entecavir
shHBV
siCtrl
siHBV1
siHBV2

G
Core
(Cytoplasmatic+ cells/mm²)
0.0095
0.0030
0.0050
0.0012
- ETV shHBV Ctrl HBV1 HBV2
siRNA

H
Intrahepatic HBV DNA
(copies/cell)
0.0053
0.0015
0.0033
0.0047
- ETV shHBV Ctrl HBV1 HBV2
siRNA

Figure 5

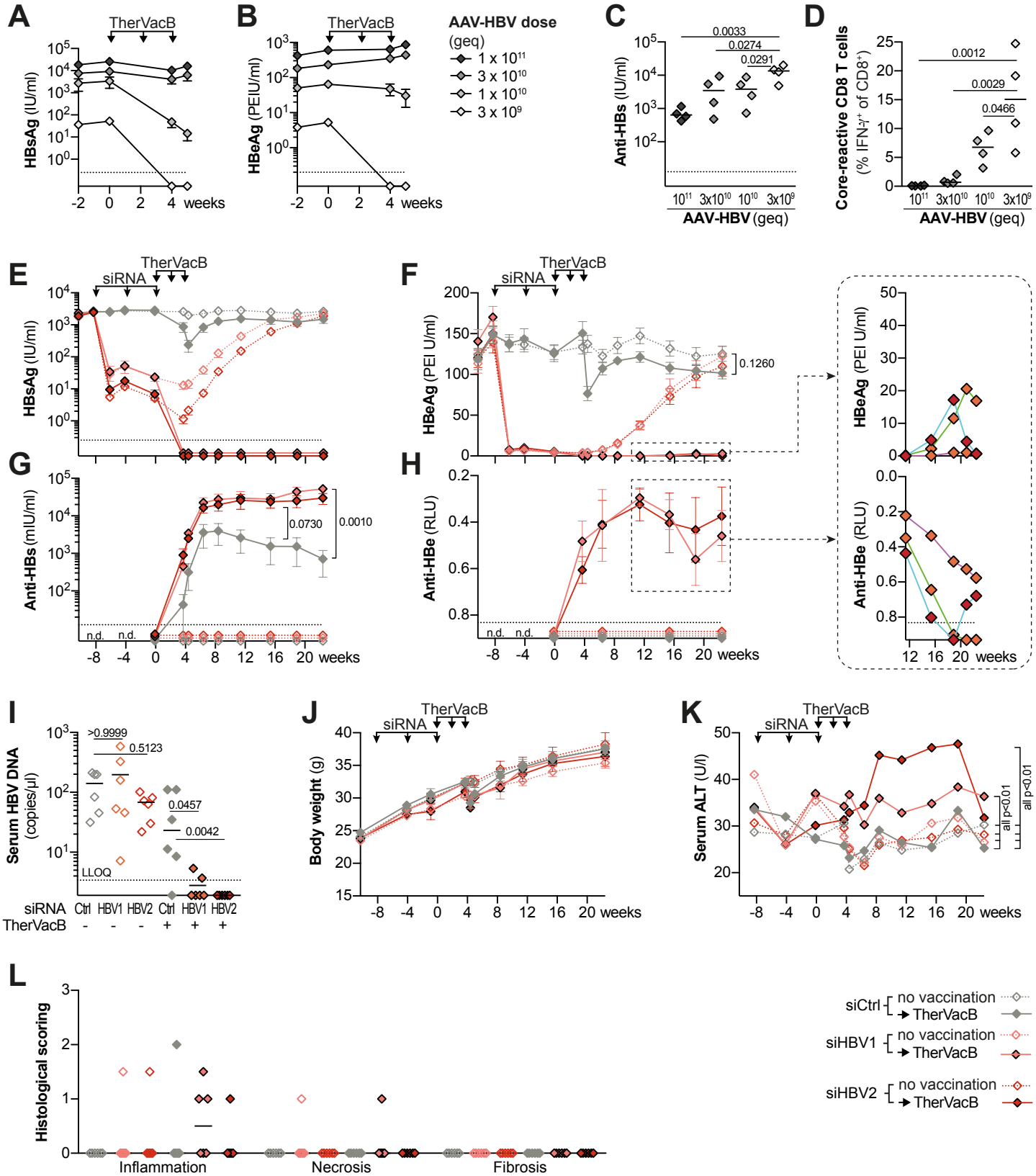
A
TherVacB
HBsAg (IU/ml)
weeks
B
TherVacB
HBeAg (PEIU/ml)
weeks
AAV-HBV dose
(geq)
1 x 10^11
3 x 10^10
1 x 10^10
3 x 10^9
C
Anti-HBs (IU/ml)
0.0033
0.0274
0.0291
AAV-HBV (geq)
D
Core-reactive CD8 T cells
(% IFN-γ+ of CD8+)
0.0012
0.0029
0.0466
AAV-HBV (geq)
E
TherVacB
siRNA
HBsAg (IU/ml)
F
TherVacB
siRNA
HBeAg (PEI U/ml)
0.1260
G
Anti-HBs (mIU/ml)
0.0730
0.0010
n.d.
weeks
H
Anti-HBe (RLU)
n.d.
weeks
HBeAg (PEI U/ml)
Anti-HBe (RLU)
weeks
I
Serum HBV DNA
(copies/µl)
>0.9999
0.5123
0.0457
0.0042
LLOQ
siRNA Ctrl HBV1 HBV2 Ctrl HBV1 HBV2
TherVacB - - - + + +
J
TherVacB
siRNA
Body weight (g)
weeks
K
TherVacB
siRNA
Serum ALT (U/l)
all p<0.01
all p<0.01
weeks
L
Histological scoring
Inflammation
Necrosis
Fibrosis
siCtrl no vaccination → TherVacB
siHBV1 no vaccination → TherVacB
siHBV2 no vaccination → TherVacB

Figure 6

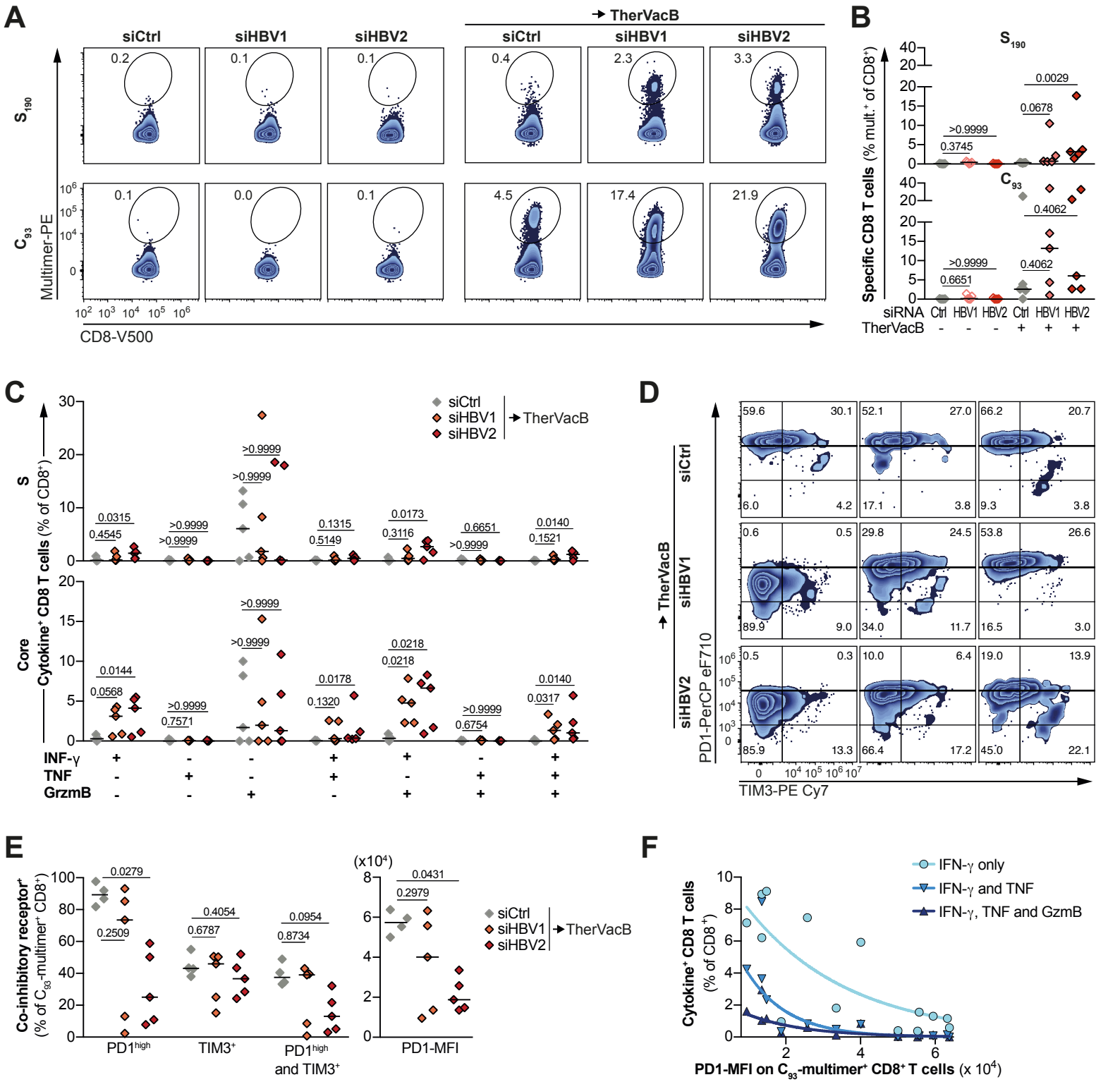
A
siCtrl
siHBV1
siHBV2
TherVacB
S190
C93
Multimer-PE
CD8-V500
B
Specific CD8 T cells (% mult.+ of CD8+)
siRNA Ctrl HBV1 HBV2 Ctrl HBV1 HBV2
TherVacB - - - + + +
C
S
Core
Cytokine+ CD8 T cells (% of CD8+)
INF-γ
TNF
GrzmB
D
PD1-PerCP eF710
TIM3-PE Cy7
E
Co-inhibitory receptor+ (% of C93-multimer+ CD8+)
PD1high
TIM3+
PD1high and TIM3+
PD1-MFI
F
Cytokine+ CD8 T cells (% of CD8+)
IFN-γ only
IFN-γ and TNF
IFN-γ, TNF and GzmB
PD1-MFI on C93-multimer+ CD8+ T cells (x 10^4)

Figure 7

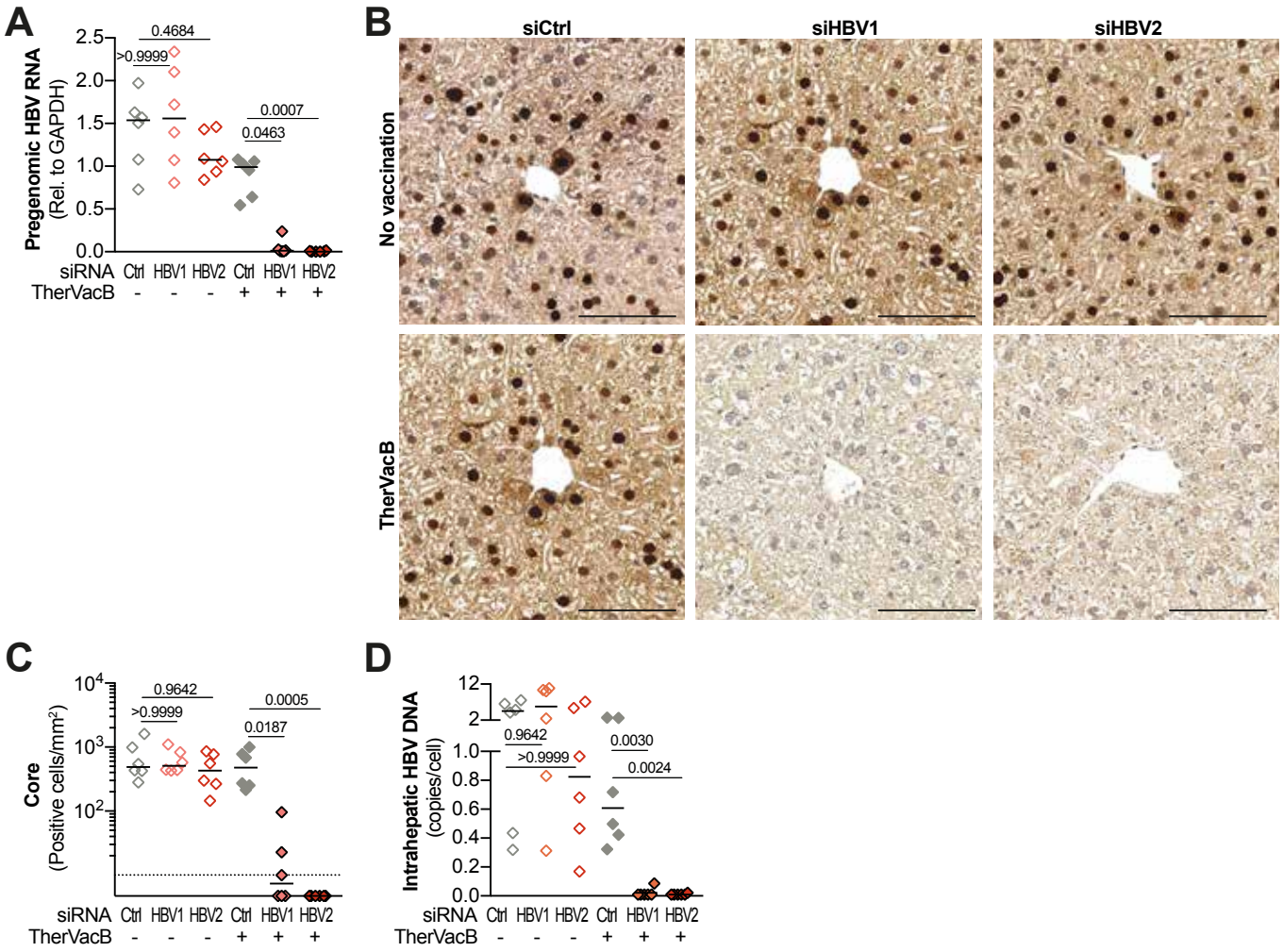
A
Pregenomic HBV RNA
(Rel. to GAPDH)
2.5
2.0
1.5
1.0
0.5
0.0
0.4684
>0.9999
0.0007
0.0463
siRNA Ctrl HBV1 HBV2 Ctrl HBV1 HBV2
TherVacB - - - + + +
B
siCtrl
siHBV1
siHBV2
No vaccination
TherVacB
C
Core
(Positive cells/mm²)
10⁴
10³
10²
0.9642
>0.9999
0.0005
0.0187
siRNA Ctrl HBV1 HBV2 Ctrl HBV1 HBV2
TherVacB - - - + + +
D
Intrahepatic HBV DNA
(copies/cell)
12
2
1.0
0.8
0.6
0.4
0.2
0.0
0.9642
>0.9999
0.0030
0.0024
siRNA Ctrl HBV1 HBV2 Ctrl HBV1 HBV2
TherVacB - - - + + +

Figure S1

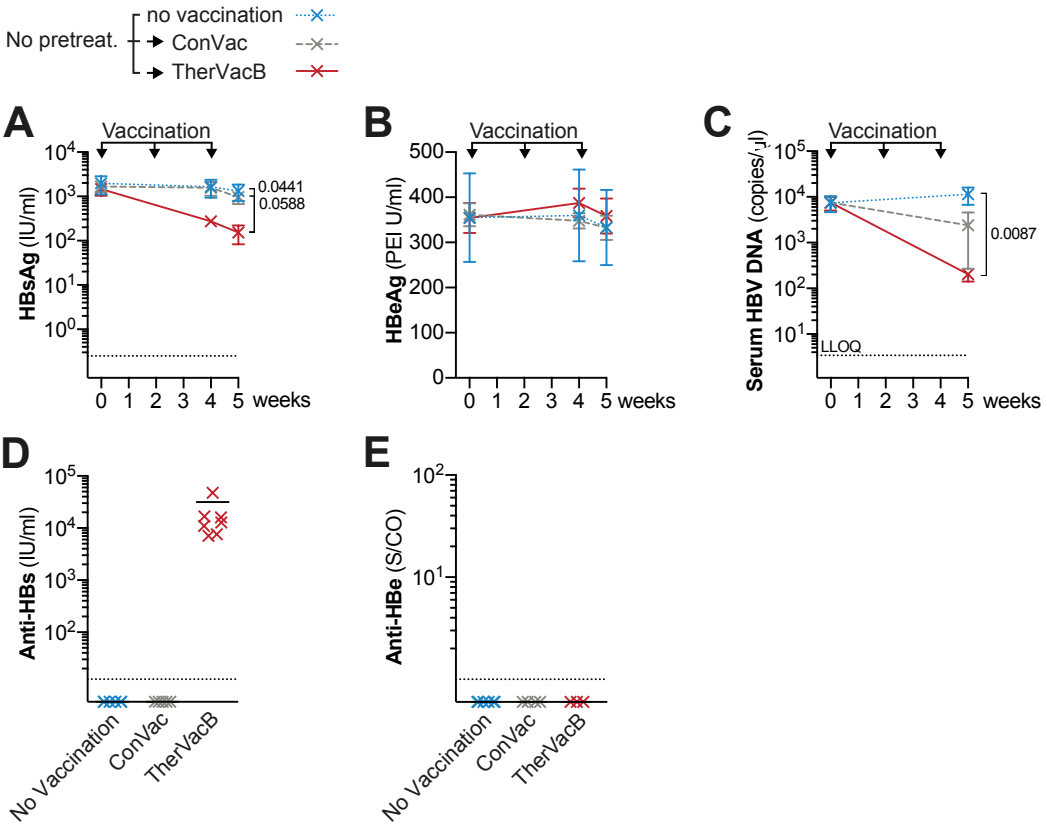
No pretreat.
no vaccination
ConVac
TherVacB
A
Vaccination
HBsAg (IU/ml)
0.0441
0.0588
weeks
B
Vaccination
HBeAg (PEI U/ml)
weeks
C
Vaccination
Serum HBV DNA (copies/μl)
0.0087
LLOQ
weeks
D
Anti-HBs (IU/ml)
No Vaccination
ConVac
TherVacB
E
Anti-HBe (S/CO)
No Vaccination
ConVac
TherVacB

Figure S2

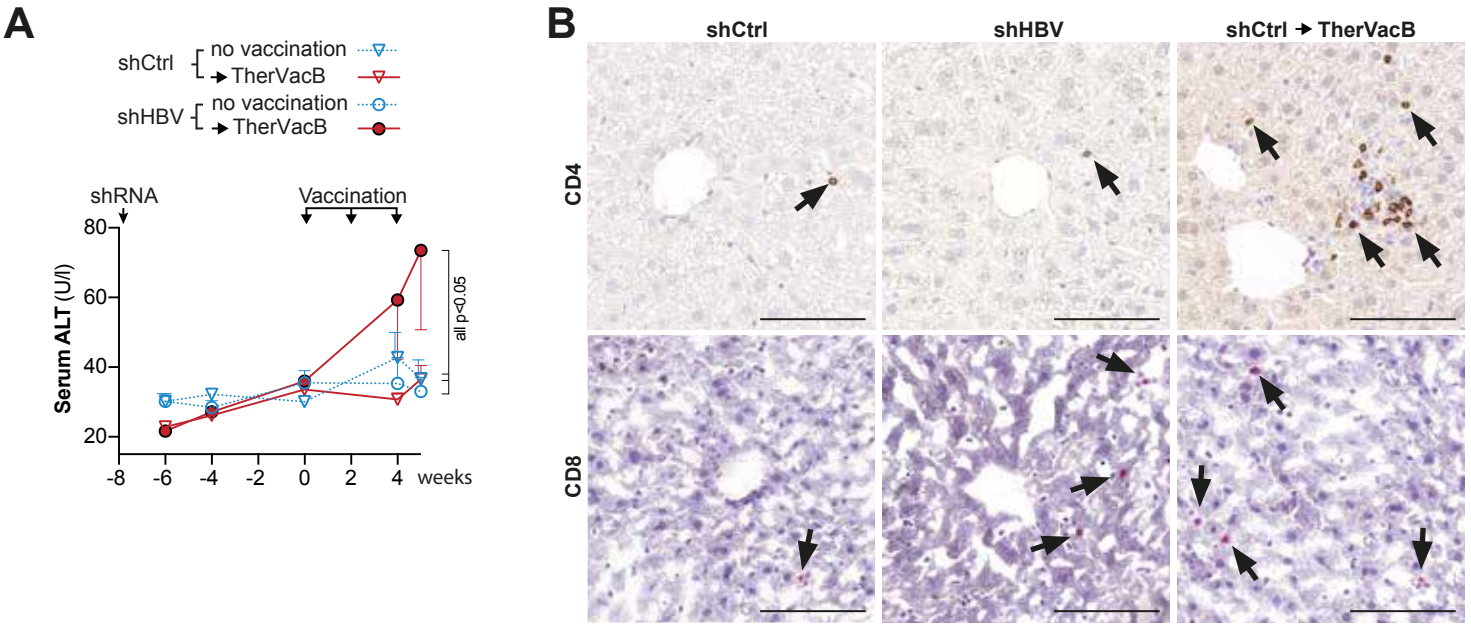
A
shCtrl
no vaccination
TherVacB
shHBV
no vaccination
TherVacB
shRNA
Vaccination
Serum ALT (U/l)
80
60
40
20
-8
-6
-4
-2
0
2
4
weeks
all p<0.05
B
shCtrl
shHBV
shCtrl → TherVacB
CD4
CD8

Figure S3

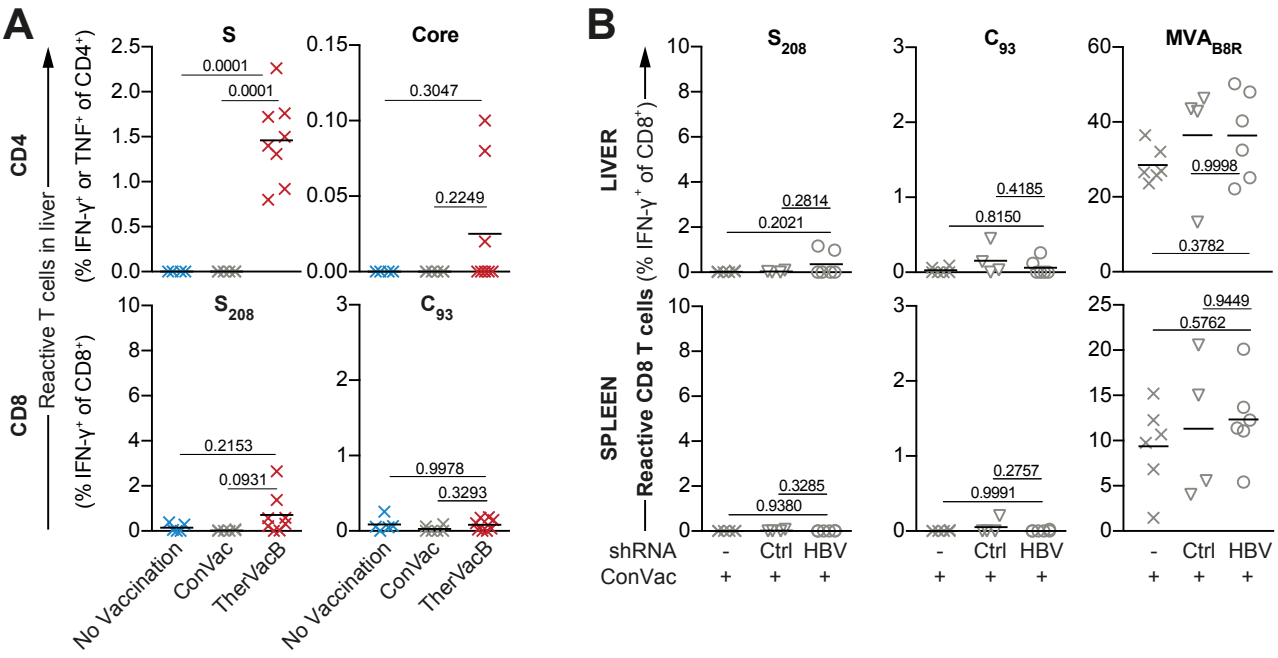
A
CD4
CD8
Reactive T cells in liver
(% IFN-γ+ or TNF+ of CD4+)
(% IFN-γ+ of CD8+)
S
Core
S208
C93
0.0001
0.0001
0.3047
0.2249
0.2153
0.0931
0.9978
0.3293
No Vaccination
ConVac
TherVacB
B
LIVER
SPLEEN
Reactive CD8 T cells (% IFN-γ+ of CD8+)
S208
C93
MVAB8R
0.2814
0.2021
0.4185
0.8150
0.9998
0.3782
0.3285
0.9380
0.2757
0.9991
0.9449
0.5762
shRNA - Ctrl HBV
ConVac + + +

Figure S4

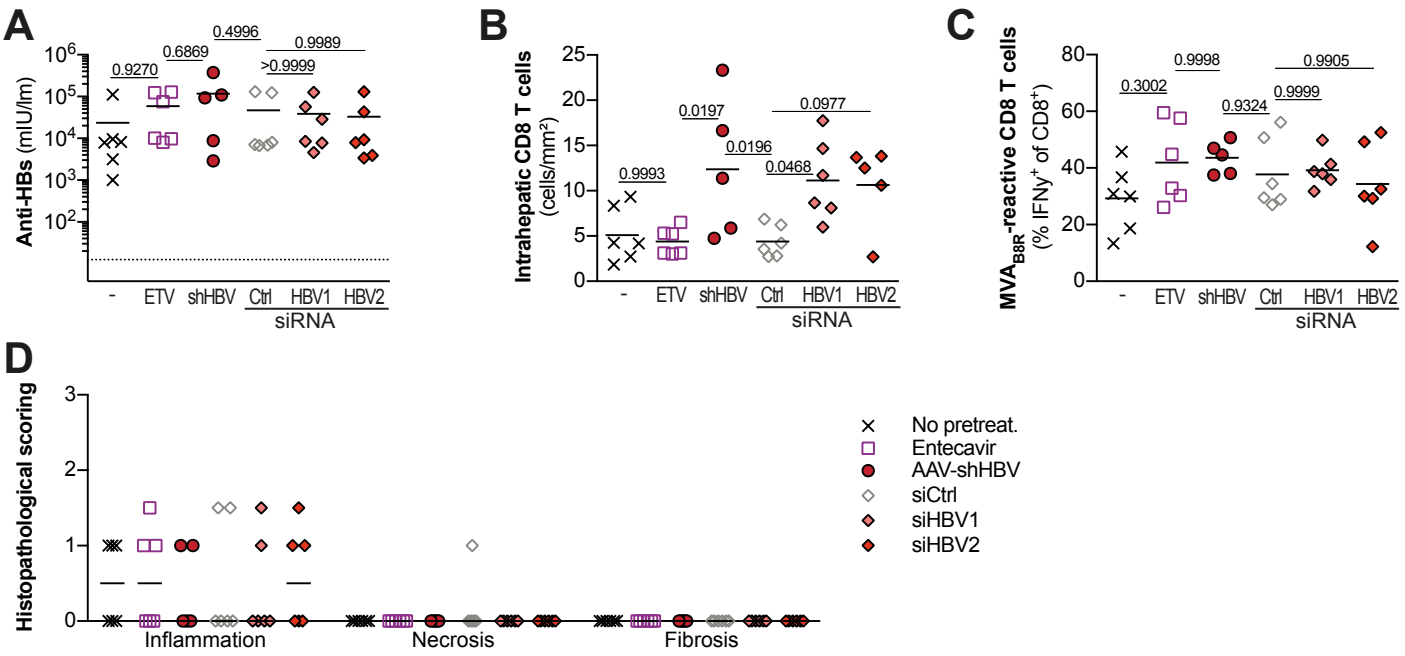
A
Anti-HBs (mIU/lm)
0.9270
0.6869
0.4996
>0.9999
0.9989
B
Intrahepatic CD8 T cells (cells/mm²)
0.9993
0.0197
0.0196
0.0468
0.0977
C
MVA$_{B8R}$-reactive CD8 T cells (% IFNγ$^+$ of CD8$^+$)
0.3002
0.9998
0.9324
0.9999
0.9905
- ETV shHBV Ctrl HBV1 HBV2
siRNA

D
Histopathological scoring
Inflammation
Necrosis
Fibrosis
No pretreat.
Entecavir
AAV-shHBV
siCtrl
siHBV1
siHBV2

Figure S5

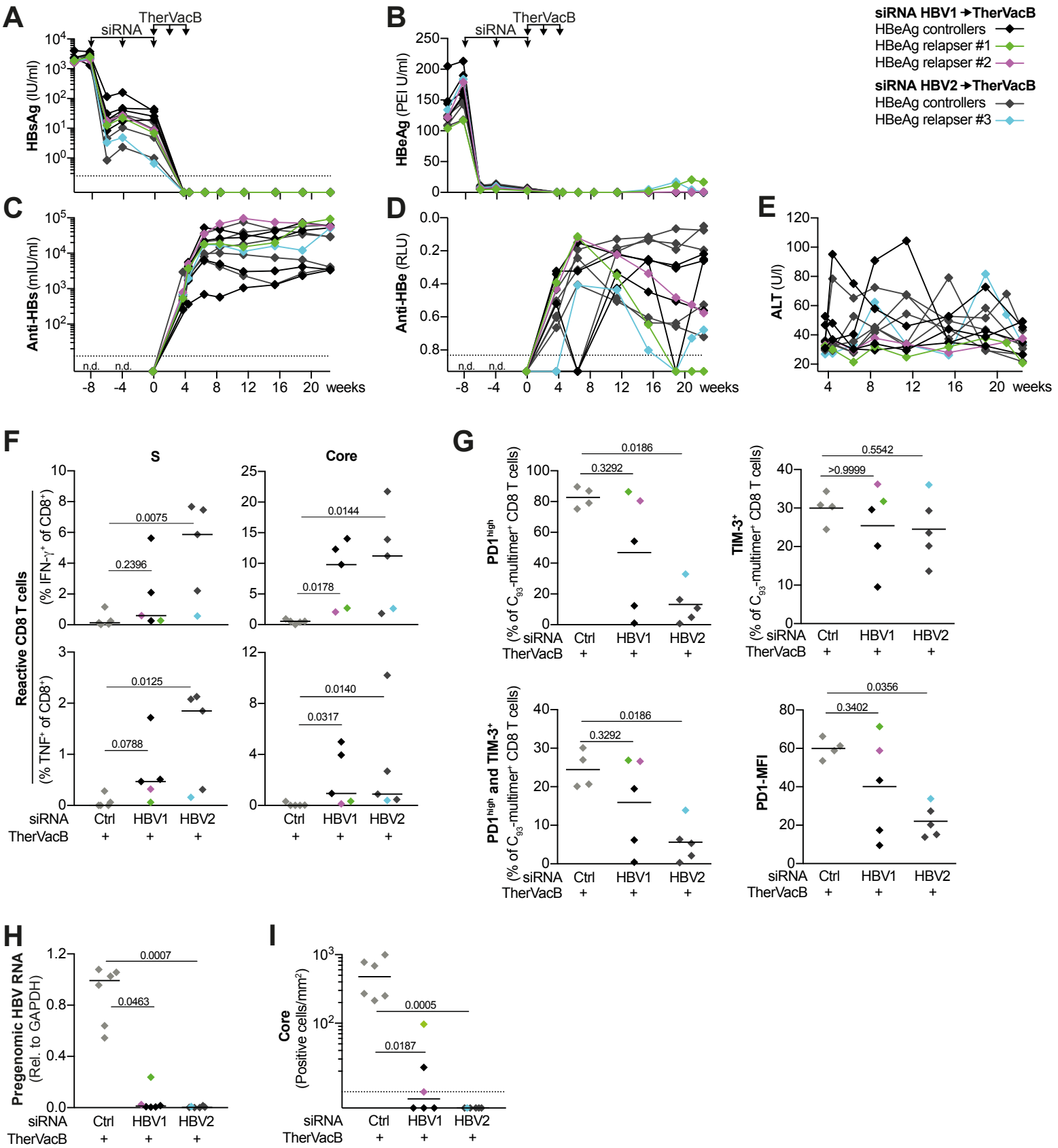
A
TherVacB
siRNA
HBsAg (IU/ml)
B
HBeAg (PEI U/ml)
siRNA HBV1 → TherVacB
HBeAg controllers
HBeAg relapser #1
HBeAg relapser #2
siRNA HBV2 → TherVacB
HBeAg controllers
HBeAg relapser #3
C
Anti-HBs (mIU/ml)
n.d.
weeks
D
Anti-HBe (RLU)
E
ALT (U/l)
F
S
Core
Reactive CD8 T cells
(% IFN-γ+ of CD8+)
(% TNF+ of CD8+)
0.0075
0.2396
0.0144
0.0178
0.0125
0.0788
0.0140
0.0317
siRNA
TherVacB
Ctrl
HBV1
HBV2
G
PD1high
(% of C93-multimer+ CD8 T cells)
0.0186
0.3292
TIM-3+
0.5542
>0.9999
PD1high and TIM-3+
PD1-MFI
0.0356
0.3402
H
Pregenomic HBV RNA
(Rel. to GAPDH)
0.0007
0.0463
I
Core
(Positive cells/mm2)
0.0005
0.0187

Figure S6

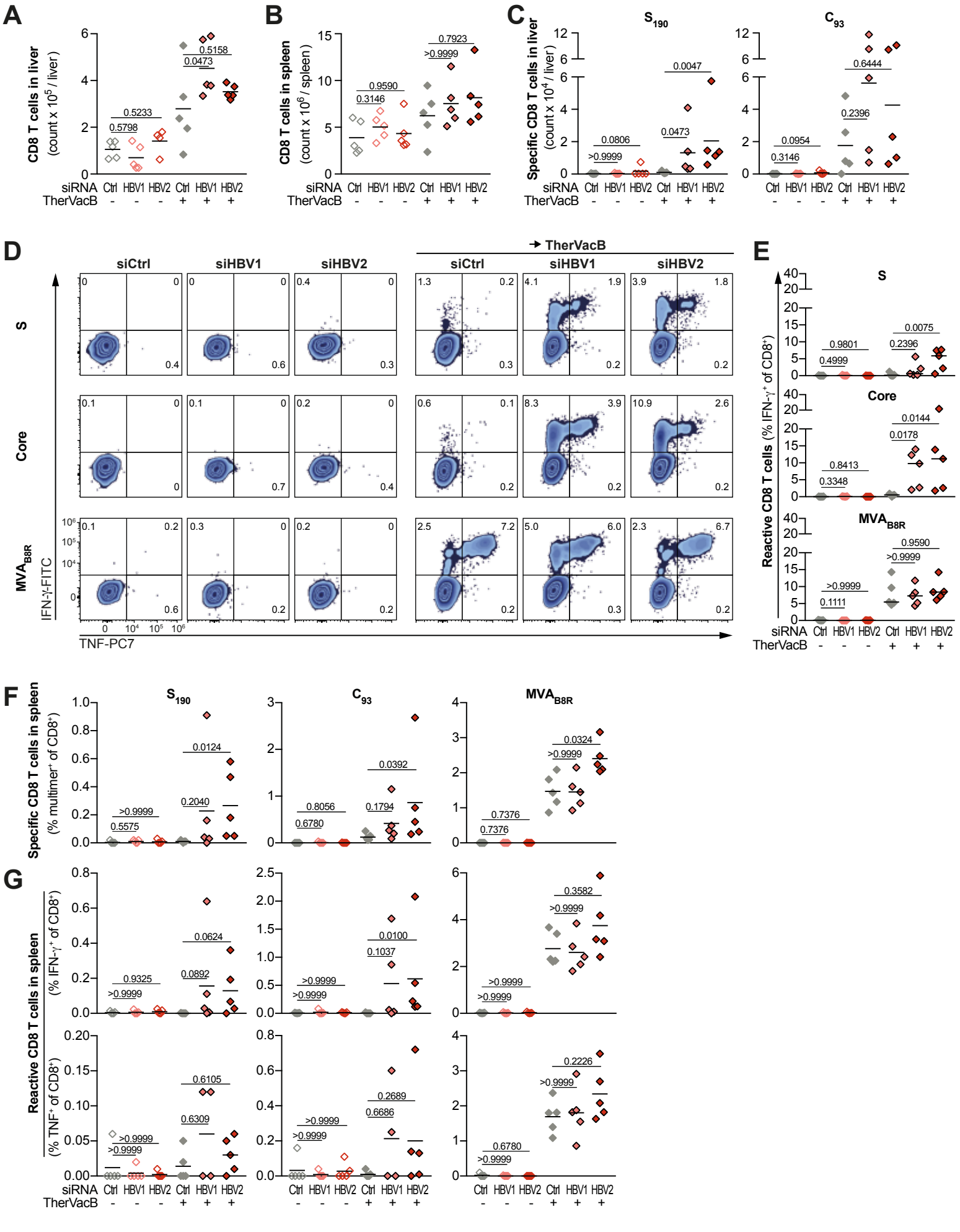
A
CD8 T cells in liver
(count x 10^5 / liver)
B
CD8 T cells in spleen
(count x 10^6 / spleen)
C
Specific CD8 T cells in liver
(count x 10^4 / liver)
S190
C93
siRNA Ctrl HBV1 HBV2 Ctrl HBV1 HBV2
TherVacB - - - + + +
D
siCtrl
siHBV1
siHBV2
TherVacB
S
Core
MVAB8R
IFN-γ-FITC
TNF-PC7
E
Reactive CD8 T cells (% IFN-γ+ of CD8+)
F
Specific CD8 T cells in spleen
(% multimer+ of CD8+)
G
Reactive CD8 T cells in spleen
(% IFN-γ+ of CD8+)
(% TNF+ of CD8+)

Figure S7

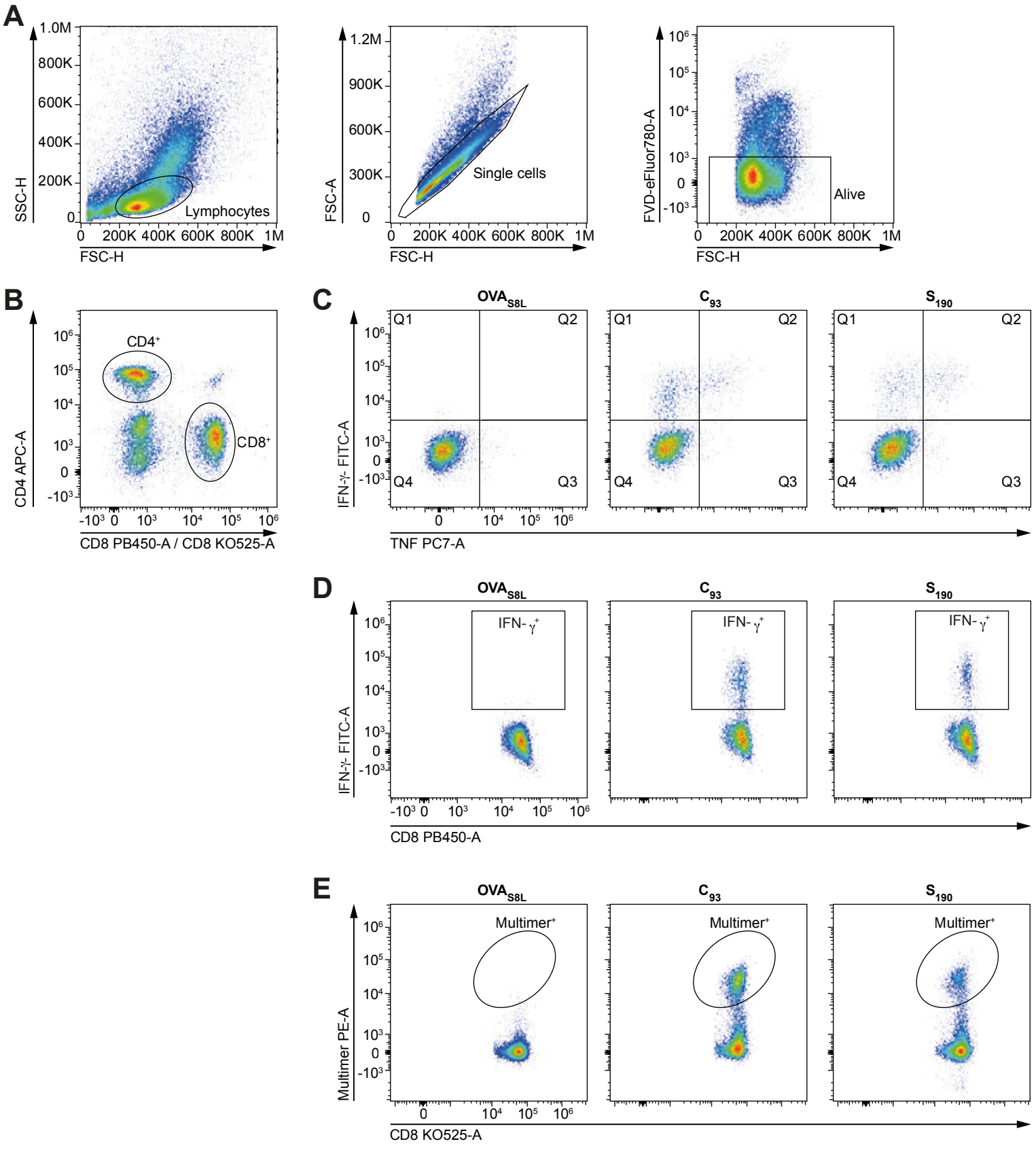
A
SSC-H
FSC-H
Lymphocytes
FSC-A
Single cells
FVD-eFluor780-A
Alive
B
CD4 APC-A
CD4+
CD8+
CD8 PB450-A / CD8 KO525-A
C
OVAS8L
C93
S190
Q1
Q2
Q3
Q4
IFN-γ- FITC-A
TNF PC7-A
D
IFN-γ+
CD8 PB450-A
E
Multimer+
Multimer PE-A
CD8 KO525-A